Lebanese American University

Assessing membrane biofilm predevelopment strategies to improve anaerobic membrane bioreactor effluent quality

By

Christelle Bou Nehme Sawaya

A Thesis

Submitted in partial fulfillment of the requirements

for the degree of Master of Science in Engineering

School of Engineering

May 2022

LAU
الجامعة اللبنانية الأميركية
Lebanese American University

THESIS APPROVAL FORM

Student Name: Christelle Bou Nehme Sawaya I.D. #: 201400942

Thesis Title : Assessing membrane biofilm predevelopment strategies to improve anaerobic membrane bioreactor effluent quality

Program: Civil and Environmental Engineering

Department: Civil Engineering

School: Engineering

The undersigned certify that they have examined the final electronic copy of this thesis and approved it in Partial Fulfillment of the requirements for the degree of:

Master of Science in the major of Civil and Environmental Engineering

Thesis Advisor's Name Moustapha Harb	Signature [redacted]	DATE: 16 / 05 / 2022 (Day / Month / Year)
Committee Member's Name Mahmoud Wazne	Signature [redacted]	DATE: 16 / 05 / 2022 (Day / Month / Year)
Committee Member's Name Sima Tokajian	Signature [redacted]	DATE: 16 / 05 / 22 (Day / Month / Year)

LAU
الجامعة اللبنانية الأميركية
Lebanese American University

THESIS COPYRIGHT RELEASE FORM

LEBANESE AMERICAN UNIVERSITY NON-EXCLUSIVE DISTRIBUTION LICENSE

By signing and submitting this license, you (the author(s) or copyright owner) grants the Lebanese American University (LAU) the non-exclusive right to reproduce, translate (as defined below), and/or distribute your submission (including the abstract) worldwide in print and electronic formats and in any medium, including but not limited to audio or video. You agree that LAU may, without changing the content, translate the submission to any medium or format for the purpose of preservation. You also agree that LAU may keep more than one copy of this submission for purposes of security, backup and preservation. You represent that the submission is your original work, and that you have the right to grant the rights contained in this license. You also represent that your submission does not, to the best of your knowledge, infringe upon anyone's copyright. If the submission contains material for which you do not hold copyright, you represent that you have obtained the unrestricted permission of the copyright owner to grant LAU the rights required by this license, and that such third-party owned material is clearly identified and acknowledged within the text or content of the submission. IF THE SUBMISSION IS BASED UPON WORK THAT HAS BEEN SPONSORED OR SUPPORTED BY AN AGENCY OR ORGANIZATION OTHER THAN LAU, YOU REPRESENT THAT YOU HAVE FULFILLED ANY RIGHT OF REVIEW OR OTHER OBLIGATIONS REQUIRED BY SUCH CONTRACT OR AGREEMENT. LAU will clearly identify your name(s) as the author(s) or owner(s) of the submission, and will not make any alteration, other than as allowed by this license, to your submission.

Name: Christelle Bou Nehme Sawaya

Signature: [redacted] Date: 16 / 05 / 2022
Day Month Year

LAU
الجامعة اللبنانية الأميركية
Lebanese American University

PLAGIARISM POLICY COMPLIANCE STATEMENT

I certify that:

1. I have read and understood LAU's Plagiarism Policy.
2. I understand that failure to comply with this Policy can lead to academic and disciplinary actions against me.
3. This work is substantially my own, and to the extent that any part of this work is not my own I have indicated that by acknowledging its sources.

Name: Christelle Bou Nehme Saliba

Signature: [redacted]

Date: 16 / 05 / 2022
Day Month Year

ACKNOWLEDGMENTS

I would like to express my gratitude to my advisor, Dr. Moustapha Harb, who guided me throughout the completion of this project and provided valuable professional assistance.

I would also like to thank the committee members, Dr. Sima Tokajian and Dr. Mahmoud Wazne, for their insights and constructive feedback on the research.

Assessing membrane biofilm predevelopment strategies to improve anaerobic membrane bioreactor effluent quality

Christelle Bou Nehme Sawaya

ABSTRACT

Recycling and reuse of treated wastewater has been addressed as an alternative water resource to a great extent lately because of major water scarcity faced worldwide. Among wastewater treatment technologies envisaged, anaerobic membrane bioreactors (AnMBRs) have demonstrated considerable benefits for high quality effluent and energy recovery. Specifically, recent developments in the understanding of membrane biofilms in AnMBRs indicate additional advantages to their known benefits as an emerging technology. In addition to high COD removal, increased biogas production and lower energy costs, AnMBRs are found to play a key role for the degradation of emerging contaminants of concern. The present work aimed to determine the effect of combining different membrane biofilm development conditions in an AnMBR on effluent quality, trimethoprim removal, antibiotic resistance genes (ARGs) proliferation, and effluent methane concentrations. The experiment consisted of two phases during which membrane biofilms were initially developed at different transmembrane pressures (TMPs) by varying the membrane flux rates and subsequently operated at the same flux rate for performance comparison. The first phase consisted of membrane biofilm development at low flux rate while the second phase was devised to allow membrane biofilm development at high flux rate. Improved performance was observed for a membrane on which the biofilm was initially developed at high TMP. After reduction of flux, lower TMP was sustained for the same membrane, on which higher COD and trimethoprim removals were observed. Analysis of membrane biofilm communities revealed presence of specific groups, notably methanogens and their associated syntrophic groups that confer benefits to effluent quality. Moreover, a remarkable difference between the microbial groups of the membrane biofilm layers developed at high TMP was observed. This study highlights a new approach for controlled membrane biofilm operation that can potentially promote water quality and micropollutant removal.

Keywords: Antibiotic, Microbial Community, Micropollutant, Membrane Biofilm, AnMBR.

Table of Contents

List of Figures

List of Tables

List of Abbreviations

AD	anaerobic digestion
AeMBR	aerobic membrane bioreactor
AnMBR	anaerobic membrane bioreactor
ATP	adenosine triphosphate
ARG	antibiotic resistance gene
COD	chemical oxygen demand
CSTR	continuously stirred tank reactor
EDG	electron-donating group
EPS	extracellular polymeric substances
EWG	electron-withdrawing group
HRT	hydraulic retention time
LC-MS	liquid chromatography mass spectrometry
LRV	log removal value
MBR	membrane bioreactor
MF	microfiltration
MW	molecular weight
NCBI	National Center for Biotechnology Information
NOB	nitrite-oxidizing bacteria
OMP	organic micropollutant
OTU	operational taxonomic unit
PBS	phosphate buffered saline
PCoA	principal coordinate analysis
PVDF	polyvinylidene fluoride
qPCR	quantitative polymerase chain reaction
RDP	ribosomal database project
SRB	sulfate reducing bacteria
SRT	solids retention time
SMP	soluble microbial products
TMP	transmembrane pressure
WWTPs	wastewater treatment plants

Chapter One

Introduction

1.1. Anaerobic Membrane Bioreactor: Emerging Technology

The growth of the world's population and the mismanagement of water resources have led to scarcity of water to become a serious issue. Even though water availability is expected to increase with the climate change causing additional environmental problems, the concept of water footprint has been growing ever since (Jeswani et al., 2011). For that matter, the concept of wastewater reuse has been adopted lately, leading to its effective treatment as an importance factor to ensure appropriate water quality, that confirms to regulations and standards, is discharged mainstream. Activated sludge, commonly employed for secondary wastewater treatment, has been the basis of several emerging technologies developed such as the membrane bioreactor (MBR). However, considering that current treatments are energy intensive, a shift towards anaerobic treatment has gained popularity in recent years (Jeswani et al., 2011; Smith et al., 2012).

The need for sustainable development and effective wastewater treatment have led to a surge in biotechnology research, among which is the membrane bioreactor (MBR). The treatment process combines membrane separation and biological treatment. The system is able to completely separate solid - liquid phases independently of other factors such as sludge properties and biological process conditions (Ng et al., 2006). Compared to conventional wastewater treatments, MBRs have been established as a reliable technology with great efficiency for enhanced water quality through particle free effluent with the possibility of water reuse with minimal post-treatment required

(Jefferson et al., 2000). Among the advantages attributed to MBRs is the long sludge retention times (SRT) that prevents the washout of organisms that are capable of degrading complex organic contaminants. The separation of the hydraulic retention time, HRT and SRT, enables high feeding rate with smaller digester volumes with the production of a smaller digested sludge volume with the operation of longer SRT and shorter HRT (Dagnew et al., 2021). While the system has been applied for both aerobic and anaerobic treatments, anaerobic MBRs, AnMBRs, have proven to have greater benefits in terms of lower operating costs because of no continuous aeration requirements, lower sludge losses, and energy recovery in the form of methane (Baek et al., 2006).

The anaerobic membrane bioreactor (AnMBR) is based on the anaerobic digestion (AD) method which has been thoroughly studied and proven to be highly reliable for wastewater treatment through microbiological processes. The method is found to be an important driver for biogas production from different organic feedstocks, and ever since attracted researchers greatly (Verbeeck et al., 2018). It involves four steps of biochemical processes by microorganisms that are able to convert organic compounds into methane and carbon dioxide (CO_2) (Ileleji et al., 2015). It includes a large set of microbial community such as hydrolytic, acidogenic, and acetogenic bacteria, and other methanogens that belong to archaea. Ever since, many strategies were thoroughly studied to enhance its application and improve biogas yield and effluent quality for reuse (Mao et al., 2015). For that instance, AnMBRs have gained wide popularity in their application to different waste streams, which include low and high strength wastewaters such as municipal and food processing and have been proven greatly beneficial.

AnMBRs are usually designed as continuously stirred tank reactors (CSTR) models and have two configurations based on their membrane units design, either as submerged or external cross-flow (Figure 1). Although external cross-flow membranes require more energy for recirculation, their advantage rely in a cross-flow shear of higher velocity as well as membrane unit accessibility. The types of membranes employed for AnMBRs configurations are flat sheet or hollow fiber membranes. Moreover, the most important design parameters considered for the AnMBR are the organic loading rate, the hydraulic retention time, and the membrane flux. For operating conditions, the factors affecting the effective biodigestion in the system include the pH value, temperature of the reactor, the loading rate, and the seeding (Jain et al., 2015). For active biodigestion, a pH maintained between 6.5 and 7.5 is required in the digestor, otherwise, the activity of methanogenic organisms is hindered. The temperature zones of the AnMBR for effective anaerobic digestion are found to be optimum at 35 ℃ for mesophilic and 55 ℃ for thermophilic (Kim et al., 2002). However, since temperature affects greatly bacterial activity, it must be noted that sudden deviations in the operating temperature could alternate the performance of the digester. Based on these conditions and design parameters, the advancement of the technology has been the interest of optimizing the application of AnMBRs for sustainable wastewater treatment and several works focused on studying the effluent quality for recycling of water.

Wastewater treatment using AnMBRs have been demonstrated as a prominent water source for various applications. Although AnMBRs do not remove nitrogen or phosphorous contents, the nutrient rich effluent could be used for agricultural irrigation. Further alleviated tertiary treatments could be envisaged for other non-potable water uses such as urban, industrial, and reclaimed wastewater (Miller,

2006). However, direct water concerns have been raised in terms of microbial pathogens, emerging micropollutants, antibiotics spread, and antibiotic resistance genes (ARGs) proliferation in the effluent because such systems are not usually designed for their removal. Their presence could eventually inhibit the safe discharge of water post-treatment and cause harm to humans and plants (Harb et al., 2017). Another challenge facing the application of AnMBRs and thus limiting its implementation to full-scale is the sustainability of operational parameters such as membrane fouling, transmembrane pressure, and dissolved methane (Lui et al., 2014; Smith et al., 2012). Nevertheless, as more work is done regarding the sustainability of the AnMBR process, positive aspects of membrane biofouling mechanisms are gaining more attraction and are the focus of future work.

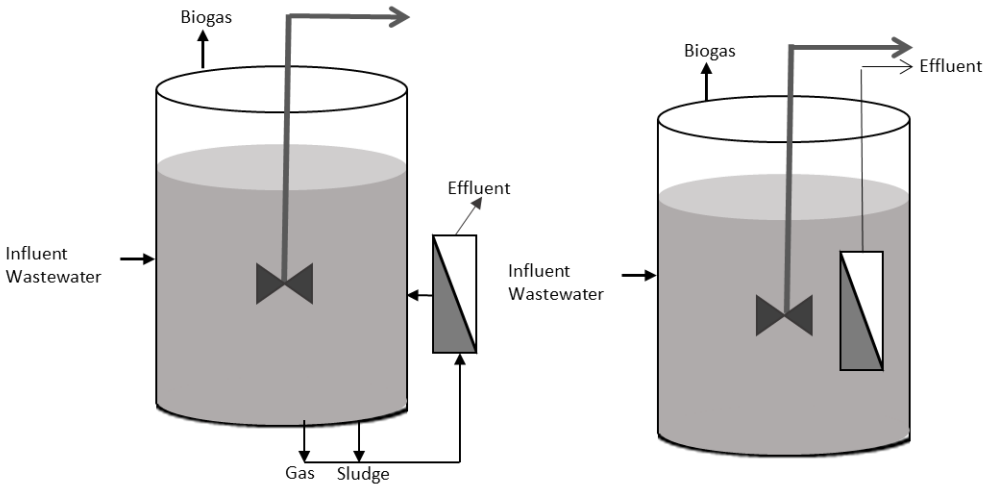

Figure 1 AnMBRs membranes configurations: (A) submerged and (B) external cross-flow.

1.2. Background: Anaerobic Membrane Biofilm

In an AnMBR, considerable biomass is in contact with the membrane and biomass growth along with soluble microbial products (SMP) and extracellular polymeric substances (EPS) deposition on the surface of the membrane (Liao et al., 2006). Such products are capable of aggregation and formation of a biofilm on the surface of the membrane (Figure 2). Fouling dynamics have been extensively studied, and descriptions behind fouling modes are reported as intermediate or complete pore blockage and cake formation (Charfi et al., 2012). The problem resulting from membrane fouling is the increase in membrane resistance through increased transmembrane pressure and subsequent decrease in membrane flux. Although research focused on controlling membrane fouling for sustainable MBR operations, mostly AeMBRs, it is not until recently that fouling on anaerobic membrane has been found to possess key differences from that of aerobic membranes. In addition, it was observed that biofilm doesn't necessarily correlate with TMP in AnMBR (Harb et al., 2019).

The difference in formation of biofilm is based on microbial groups, micro-particles, and soluble microbial products, which confer potential advantages attributed to AnMBRs. Indeed, these benefits include the reduction and removal of emerging contaminants, namely, organic micropollutants (OMPs) and antibiotic resistance genes (ARGs) (Sanguanpak et al., 2019; Yao et al., 2020). Thus, a major factor not to be overlooked in membrane biofilms dynamics is the presence of inherent microbial communities in anaerobic membrane biofilms. In addition, A recent review discussed the basis of biofilm removal mechanisms, which includes retention of the membrane fouling layer and adsorption onto extracellular polymeric substance matrix, and ultimately biodegradation by anaerobic biofilm specific microorganisms (BouNehme

Sawaya and Harb 2021). Indeed, AnMBRs rely on different biological processes than AeMBRs and key microbial communities including fermentative, methanogenic, and syntrophic groups were reported to dominate membrane biofouling layers in such systems (Cheng et al., 2019). Among the genera included are *Acinetobacter, Geobacter, Methanothrix, Syntrophomonas,* etc. Additionally, such groups were associated with anaerobic degradation of emerging contaminants and have also been observed as present in notably different relative abundances than those found in the suspended anaerobic sludge (Harb et al., 2015).

The removal mechanisms behind anaerobic membrane biofilms depend on the properties of the organic micropollutants (OMPs) and ARGs subtypes (Figure 3). For instance, hydrophobic OMPs are adsorbed onto the membrane biofilm and their biodegradation can be promoted by the microbial consortium. On the other hand, hydrophilic OMPs would be either biodegraded by the AnMBRs suspended sludge or rejected by the membrane biofilm but with the formation of a denser biofilm with micro-particles not greater than 0.1 µm. Considering that ARGs are found as intracellular (inside bacterial cells) and extracellular (outside bacterial cells) because of their dynamic proliferation nature, their total removal will be based on the removal of each subtype combined. Compared to aerobic biomass, AnMBRs are found to have lower overall ARGs abundance in the suspended biomass and for intracellular ARGs, membrane biofilms have a reduced release rate of ARGs-containing bacterial cells. For extracellular ARGs however, a denser biofilm is more advantageous in promoting refractory retention by the biofouling layer (Bou Nehme Sawaya and Harb, 2021).

As anaerobic membrane biofilms haven’t been thoroughly studied yet, targeted research is still required to unlock the potential of the biofouling layer. An increased

understanding of the interaction between key microbial groups, biofilm formation mechanisms, and biodegradation mechanisms is required to devise effective strategies for biofilm development. It is noteworthy that transmembrane pressure and flux rate parameters of the AnMBR are greatly involved in the process to prevent the hinderance of the system. No previous work assessed the effect of developing an anaerobic membrane biofilm with varying TMPs. Thus, two development strategies were devised consecutively in the experimental work presented for the membrane biofilm formation in the AnMBR and its performance assessment.

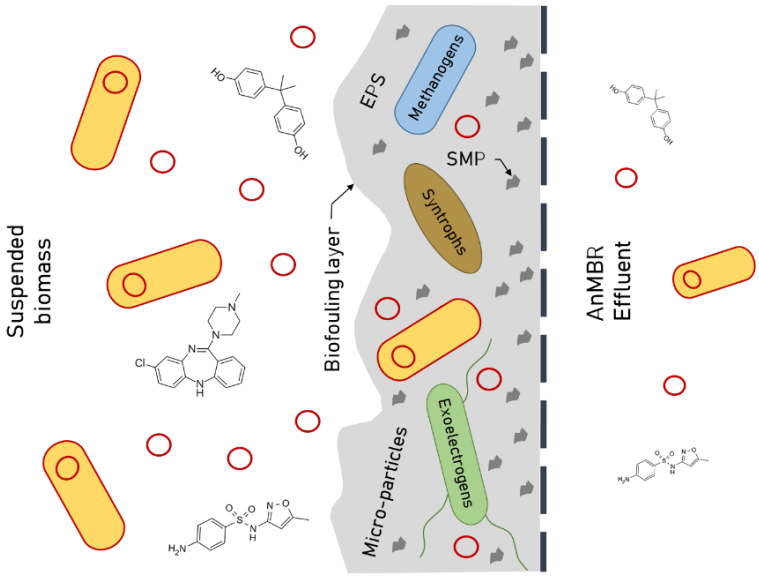

Figure 2 Schematic representation of membrane biofilm components and microbial communities (Bou Nehme Sawaya and Harb, 2021).

EC	EC Subtype	Primary Basis of Biofilm Removal	
Organic Micropollutants (OMPs)	Hydrophobic OMPs	Adsorption onto extracellular polymeric substance matrix and subsequent biodegradation	Dominance of anaerobic biofilm microbial communities by key OMP-degrading groups
	Hydrophilic OMPs	Refractory retention caused by membrane fouling layer and improved sludge biodegradation	Higher biofilm density caused by EPS, SMP, and/or Micro-particles
Antibiotic Resistance Genes (ARGs)	Intracellular ARGs	Reduced rate of release of ARG-containing bacterial cells	Lower overall ARG abundances in anaerobic biomass compared to aerobic biomass
	Extracellular ARGs	Refractory retention caused by membrane fouling layer	Higher biofilm density caused by EPS, SMP, or Micro-particles

Figure 3 Emerging contaminant (EC) types and subtypes categorized based on their primary basis for biofilm-based removal, and the possible advantages to their removal by AnMBR systems.

Chapter Two

Literature Review

2.1. Biofouling in Anaerobic Membrane Bioreactors

The study of membrane biofilm formation revealed that the main fouling agents are EPS and SMP that deposit on the membrane surface, resulting in cake layer formation or pore blockage. For a cake, foulant layers deposit on the surface of the membrane, whereas in the case of pore blockage, foulants adsorb internally in the membrane (Vrouwenvelder et al., 2010). It has been reported that in cross-flow microfiltration, sludge components are deposited through two opposite forces, which include the permeation drag and shear forces by back transport velocity (Belfort et al., 1994). With increased permeate flux, TMP increases, resulting in higher permeation drag. Thus, the negative effects of membrane fouling in MBRs generally have been linked to increased transmembrane pressure.

In their study, for example, Hwang et al. correlated TMP increases and the sudden increase in EPS concentrations in the cake layer on the membrane surface of submerged membranes in an aerobic tank (Hwang et al., 2008). However, significant work dedicated to understanding fouling mechanisms on AnMBRs found that the fouling mechanisms are not necessarily similar to AeMBRs. For that matter, Xiong et al. illustrated the fouling mechanisms differences between AeMBRs and AnMBRs under similar operating conditions and the same reactor configurations. The characterization of molecular weight (MW) fingerprint profiles revealed that SMP products and soluble EPS contents were correlated with anaerobic membrane fouling, namely glycolipoprotein. In contrast, adenosine triphosphate (ATP) contents were

greatly higher on the AeMBR biocake layer and no soluble EPS fragments were found in the AeMBR reactor (Xiong et al., 2016).

Among the main components of EPS, proteins concentrations were higher in soluble EPS-AnMBR. The fouling mechanisms differences reported in the study highlighted the need to distinguish the fouling mechanisms between both systems with the focus of AnMBRs fouling mechanisms to understand their further properties. Fouling behaviors of SMPs and EPS were then studied specifically for a submerged anaerobic membrane bioreactor by Chen et al. Their study focused on the determination of the SMP and EPS properties and their distribution of the membrane surface in relation with the OLR of the system. Their results explained the adhesion forces responsible for the formation of cake layers linked to the hydrophobicity of proteins. At higher OLRs, with increased TMP, more soluble EPS were observed and resulted in a cake layer formation because of increased adhesion forces. At lower OLRs, however, small amounts of EPS and SMP tended to be hydrophilic and intermolecular electrostatic repulsion dominated, thus likely contributed to pore blockage (Chen et al., 2017). This study contributed to a better understanding of the mechanisms behind the fouling behavior in AnMBRs. Although a similar study found similar results in terms of cohesion interactions of EPS fractions from cake sludge in a mesophilic anaerobic membrane bioreactor, the effects of EPS and SMP accumulation were negatively reported following a decrease in the membrane flux related to higher EPS fractions retained on the membrane (Ding et al., 2015).

Considering that studies conducted on AnMBRs biofouling development are still in their early stages, interesting observations found that membranes are operable without significant increases in TMPs. Robles et al. (2020) and Gouveia (2015) for example, observed that it was possible to operate membrane units at lower TMPs at

high flux rates. More interestingly, Yao et al. (2021) proved the ability to sustain biocakes formed immediately before and after TMP jump in the AnMBR. Their study also compared fouling mechanisms between AnMBRs and AeMBRs and fouling dynamics results were compatible with previous findings reported. The percentages of cake fouling resistance were in similar ranges of 80 % after TMP jump, in both systems, whereas membrane resistance increased for the AnMBR in comparison to the AeMBR. Thus, these results dissociate the negative link between biocake formation and increased TMP. Furthermore, these findings suggest the possibility of having a cake layer without detrimental effect on the AnMBR. Yet, the effect of biofouling development on the performance of the AnMBR should not be overlooked.

In fact, another study by Smith et al. (2015) assessed a membrane biofilm performance on the COD removal and dissolved effluent methane contents for an AnMBR treating domestic wastewater under psychrophilic conditions. Promising findings were reported for the fouled membrane, which was controlled by sparging, in terms of TMP restoration to near zero without performance disruption. The permeate of the highly fouled membrane had the lowest COD and FVAs concentrations consistently but with higher dissolved effluent contents (Smith et al., 2015). These observations imply that biofilm dynamics do not solely rely on the presence of SMP and soluble EPS, but other factors contributing to the improved effluent quality should be considered.

While the importance of these studies resides in exploring an unusual concept that commonly attributes hindered performance to the AnMBR with biofouling formation, the biofilm matrix requires further attention in terms of studying the

complex interaction of all biofilm components, including microbial presence and metabolisms, in attempt to uncover the enhanced membrane performance.

2.2. Microbial Groups in AnMBRs Membrane Biofilms

Despite similar configurations between AeMBRs and AnMBRs, occurrence and relative abundance of microbial groups showed dissimilarities, in the biomass as well as the membranes. Indeed, different biological processes govern both systems and more insights combining biocake properties, as discussed earlier, with microbial groups, further revealed the presence of distinct microorganisms.

A comprehensive investigation of membrane biofilms dynamics revealed that relative abundances of species related to syntrophic groups, namely *Smithella propionica*, were higher in anaerobic membranes while the abundance of unclassified *Comamonadaceae* and unclassified *Chitinophagaceae* were higher in aerobic membranes (Xiong et al., 2016). Furthermore, analysis of sludge and biofilm samples from 13 AnMBRs specifically, identified core syntrophic, fermentative, and methanogenic groups (Cheng et al., 2019). Genera were identified in biofilm samples and included: *Acinetobacter, Geobacter, Methanothrix, Methanospirillum,* and *Methanobacterium.* Such observations are important in understanding the presence of core sludge microbiota in AnMBRs and would eventually aid in explaining their activity in membrane biofilms. However, further investigation in microbial communities between suspended and attached AnMBRs configurations highlighted the affinity of certain groups for surface attachment.

In their study, Harb et al. operated two types of AnMBRs, under similar mesophilic (35 ℃) operating conditions and characterized microbiota for comparison of attached and suspended biomass growth. Analysis of the microbial differences revealed higher

relative abundance in archaea in attached biomass samples. Syntrophic bacteria were also found with higher relative abundance in attached biomass, namely *Smithella* and *Syntrophomonas,* while *Geobacter* and *Desulfovibrio* genera also favored attached growth. The findings also suggested that the differences observed in the SMP constituents resulted from the different bacterial populations (Harb et al., 2015). This study was also among the first to address the importance of the AnMBR configuration in EPS affinity on membranes. The list of microbial groups found on biofilms is further extended by the study done by Zhou et al., in which certain sulfate-reducing groups could be enriched and are known to be potentially exoelectrogenic. However, the low abundance of certain microbiota should not be overlooked and should be given more attention. Zhang et al. studied the role of low-abundance bacteria on different biofilm membranes dynamics and operating conditions, revealing a significant change in microbial structure observed before and after TMP jump. For example, *Burkholdericeae,* as well as the genus *Bacillus,* were present at a relative abundance as low as 0.02% and 0.2%, respectively. However, they were found to play a role in biocake formation (Zhang et al., 2018). These findings indeed contribute greatly to the understanding of the biological behavior of microbial groups despite their relative abundance.

These studies share a common concept related to anaerobic microbial groups that appear to be favored in biofilms and could potentially have increased activity. Their activity is further linked to their biodegradability capabilities of organic matters and organic micropollutants, although conditions under which biofilms develop haven’t been thoroughly addressed.

2.3. Anaerobic Microbial Groups Role in OMPs Biodegradation in Membrane Biofilms

The occurrence of organic micropollutants, including pharmaceuticals, personal care products, and pesticides, have been continuously detected in wastewater treatment plants, and might be directly related to unmonitored discharge of treated wastewater in the aquatic system, which would eventually reach groundwater. More specifically, antibiotics are widely found in wastewater because of their extensive use for human and veterinary medicine (Sui et al., 2015). However, the mitigation of such compounds has been reported by their removal during wastewater treatment through adsorption, degradation, and transformation. In addition, other properties include molecular weight, electron-withdrawing groups (EWG), electron-donating group (EDG), and hydrophobicity (K_{ow}) (Hai et al., 2018). Thus, the removal efficiency of OMPs is dependent on the compound and such observations has also been reported for the case of MBRs (Vásquez et al., 2018). For example, Trinh et al. operated a full-sale MBR and observed OMPs removal of > 90 % while other OMPs, including trimethoprim and diclofenac, had removal rates lower than 68 % (Trinh et al., 2012). Although MBRs have been extensively studied for OMPs removal, the role of AnMBR specifically has yet to be explained which would improve the effluent quality of the process.

Since the removal of OMPs include biodegradation pathways, the role of microbial groups should not be overlooked. More specifically, the microbiota found in the AnMBR have been reported to play a key role in the biodegradation and biotransformation of compounds. In fact, a recent review documented the role of key anaerobic communities found in AnMBRs, highlighting the advantages of the membrane biofilm specifically It has been discussed that among those groups,

syntrophic and methanogenic consortia were dominant in the biofilms. The review also indicated further co-metabolic occurrence between methanogenic, syntrophic, and acidogenic bacteria for OMPs biodegradation, highlighting the potential advantages of membrane biofilms (BouNehme Sawaya and Harb, 2021). More specifically, Gonzalez-Gil et al. observed high OMP biotransformation in the anaerobic process associated with methanogens genera (Gonzalez-Gil et al., 2017; Gonzalez-Gil et al., 2018). On a similar note, Alvarino et al., also reported a relation between the biodegradation of sulfamethoxazole, trimethoprim, and naproxen with methanogenic activity (Alvarino et al., 2014). Furthermore, consortia known as exoelectrogens, such as *Geobacter* and *Desulfovibrio,* defined as microorganisms capable of transferring electrons outside of their cells, have also been observed on anaerobic membrane biofilms and are capable of degradation of several OMPs (Chen et al., 2020).

A recent work also examined the microbial activity of an AnMBR membrane biofilm in biotransformation of three antibiotics, sulfamethoxazole, erythromycin, and ampicillin. The three antibiotics were added at incremental concentrations and performed of the membrane and AnMBR in general were observed. Results showed higher activity of *Methanothrix, Methanomethylovorans, Syntrophaceae,* and *Desulfomonile* on the membrane biofilm of the AnMBR when compared to the suspended biomass, which have been reported to be involved in biotransformation products related to AnMBR effluents (Harb et al., 2021). This study was among the few first to investigate and compare the differences between suspended and attached biomass on antibiotics removal and their transformation products. The finding of this study, in addition to the advantages of anaerobic membranes reported, served as a motivation to explore strategies for anaerobic membrane biofilms development in

AnMBRs. Thus, several methods based on effluent flux rates variations were evaluated as part of this work.

2.4. AnMBR, Biofouling and ARG Removal

The overuse of antibiotics accelerated the spread of antibiotic resistance genes (ARGs) and is gaining more attention because of the global threat. The seriousness of the issue resides in the fact that ARGs are responsible for the dissemination of antibiotic resistance. Their occurrence is also unpredictable as they are detected in both natural and engineered environments (Viswanathan, 2014; Ventola et al., 2015). Wastewater treatment plants (WWTPs) are of no exception for that matter since high amount of ARGs have been reported in wastewaters (Baquero et al., 2008). Thus, increased attention has been raised to evaluate ARGs occurrence in WWTPs in relation to the efficiency of the treatment in dealing with ARGs prior to the discharge or reuse of the treated water.

MBR technologies have shown great potential as a sustainable water resource because of their ability to mitigate OMPs, compared to conventional wastewater treatments (Du et al., 2015). For example, the concentrations of bla_{KPC}, bla_{NDM}, bla_{SHV}, *ermB, intI1, sul1 and tetO* were found to be lower in an MBR than in conventional activated sludge system, up to 4.8 log removal value (LRV) (Le et al., 2018). Considering additionally the advantages of AnMBRs discussed earlier, it is important to understand the effect of AnMBR treatment on ARG dynamics, an area with limited studies done so far. Recently, ARG profiles investigated in the biomass and the effluent as part of an AnMBR treating three different classes of antibiotics, revealed an increasing trend in the abundance of target ARG in biomass samples,

namely *ermF, ermB, sul1, sul2, oxa-1, tetO,* as well as *intl1*.However, ARGs profiles were reported as differing than those of the effluents (Zarei-Baygi et al., 2020).

Preliminary research indicated ARG removal by AnMBR treatment to be promising. In their study, Kappell et al. observed lower cocnentrations of *ermB, tetO,* and *sul1,* in an AnMBR treating domestic primary clarifier wastewater (Kappell et al., 2018). For example, Lou et al. observed major influence of manure co-treatment on the abundance of *sul1, sul2, tetO, tetW, ermB, ermF, ampC, blaOXA-1, and blaNDM-1* as well as *intl1,* during AnMBR treatment as well as higher removal of target ARGs with increasing manure loading (Lou et al., 2020). The role of the membrane was also evaluated for its effect on ARGs, by considering increasing fouling severity and TMP effect in an AnMBR treating synthetic wastewater. Results showed that fouling achieved higher LRV compared to a new membrane and increased as fouling progressed, which resulted in higher TMPs. Furthermore, adsorption was reported to facilitate the removal of ARGs in the fouling layers (Cheng and Hong, 2017). In another study, membrane fouling studied in an AnMBR equipped with three membrane modules, was found to contribute greatly to ARGs removal, with highest results reported for the highest fouled membrane (Zarei-Baygi et al., 2020). Overall, these studies advanced insights to ARG activities and removal in AnMBR system although the role of the membrane hasn't been studied thoroughly yet. As the role of membrane biofilms is uncovering advantages in OMP and ARG mitigation strategies, the mechanisms behind ARG proliferation in such systems is still in its early stage.

Chapter Three

Aim and Objectives

3.1. Research Aim

The current study aimed at exploring membrane biofilm characteristics in an AnMBR and their associated ability to sustain low-pressure operation while improving effluent quality. Overall, the work also contributed to understanding the interactions of key anaerobic microbial groups with the fate of emerging contaminants in AnMBR systems, which ultimately decreases challenges that hinder the adoption of the AnMBR for full-scale wastewater treatment.

3.2. Research Objectives

1. Determine the best strategy to develop a membrane biofilm
    1.1. Investigate the effect of developing the membrane biofilm at low pressure
    1.2. Investigate the effect of developing the membrane biofilm at high pressure
2. Evaluate the performance of the AnMBR
    2.1. Evaluate effluent quality attributable to membrane biofilms
    2.2. Evaluate antibiotic removal by membrane biofilm
3. Examine microbial communities shifts on the different membranes
    3.1. Compare relative abundances of microbial groups in AnMBR samples
4. Determine the interaction between microbial groups in the biofilm matrix
5. Identify the best strategy for membrane biofilm development

3.3. Scope of Work

The experiment was conducted in two phases and consisted of an anaerobic membrane bioreactor system (AnMBR) treating synthetic municipal wastewater at 35 ℃. In the first phase, the AnMBR was set up with two external membrane units. A biofilm layer was allowed to develop on one of the two membranes at low flux and resulting in low transmembrane pressure, while the other membrane was left for comparison purposes. In the second phase, the AnMBR was set up with three external membrane units, on which membrane biofilms were allowed to develop at different flux rates, resulting in different transmembrane pressures. The membrane biofilms during both phases were developed during 17 days prior to their operation. During the operation phase, chemical oxygen demand (COD), effluent methane, and trimethoprim concentrations in the effluent were tested. Biomass and membranes were sampled for characterization of extracellular polysaccharides substances (EPS) and microbial communities.

Chapter Four

Methodology

4.1. Anaerobic Membrane Bioreactor Configuration

The anaerobic membrane bioreactor (AnMBR) was operated as a lab-scale continuously stirred tank reactor (CSTR), 3-L working volume (Chemglass Life Science, USA) and mixed at 200 rpm by an internal impeller. The temperature was set at 35 ℃ in the water-jacket to maintain mesophilic conditions. The experiment consisted of two consecutive phases, of which a membrane biofilm development stage followed by an operation stage for testing purposes. External cross-flow flat sheet membrane modules were connected in series to the reactor and ensuring that the membranes were exposed to similar cross-flow conditions. Microfiltration membranes were used, and they were made of polyvinylidene difluoride (PVDF) with 0.2 µm pore size (Microdyn Nadir, Germany) with an effective area of 0.057 m^2 each. No membrane regeneration procedures were carried out during both phases, but backwash was applied daily for 20 minutes by sending the permeate in the opposite direction of filtration to prevent membrane pores blockage. Headspace biogas was recirculated on the surface of the membranes that were relaxed for 60 seconds every 1 hour. The sludge that seeded the reactor was obtained from an anaerobic digestor in Lebanon and the feed consisted of synthetic wastewater at an organic loading rate between 0.9-1.2 g. COD/L-d for phases I and II, respectively. The pH was maintained at 7 and the sludge retention time (SRT) was 360 days, for both phases. During each phase, the flux rates were varied by setting different effluent pump rates, which were recirculated on standard digital peristaltic pumps (Masterflex, United

States). Transmembrane pressure (TMP) was measured daily using external pressure gauges. Based on the TMP (Pa), transmembrane flux, J (L/m^2-h), and μ as the viscosity of water at 25 ℃ (Pa.h), the total membrane resistance, R_T (m^{-1}), was calculated by: $R_T = \frac{TMP}{\mu \times J}$

4.2. **Membrane Biofilm Development Strategies**

For the development and operation stages of the membrane biofilms at different TMPs, filtration fluxes were varied during phases I and II by changing the effluent rates of the peristaltic pumps. For each phase, the membrane biofilms of each membrane were allowed to develop at different flux rates, referred to development stage, and then were operated, referred to operation stage, at the same flux rates to compare the performances. During phase I, the anaerobic membrane biofilm layer was developed at low pressure, at flux rate of 1.7 ± 0.3 L/m^2-h, while another new membrane simultaneously ran at a flux 5.2 ± 1 L/m^2-h, without prior biofilm development, for operation purposes. The HRT was 3.1 ± 0.4 days. After 17 days, the membrane biofilm pre-developed at low flux was operated at a higher flux with another new membrane on which biofilm wasn't pre-developed (Figure 4A). During phase II, the anaerobic membrane biofilm was set to high transmembrane pressure development (HPD), at a flux of 7.0 ± 0.4 L/m^2-h. For comparison purposes, two membranes were set to develop anaerobic biofilms at low transmembrane pressure (LPD), at 0.3 psi, and medium transmembrane pressure (MPD), at 1 psi, respectively

(Figure 4B). The HPD membrane was tested at lower pressure and was set at similar flux rates as the LPD and MPD membranes, at flux rates between 5.06 – 5.25 L/m^2-h.

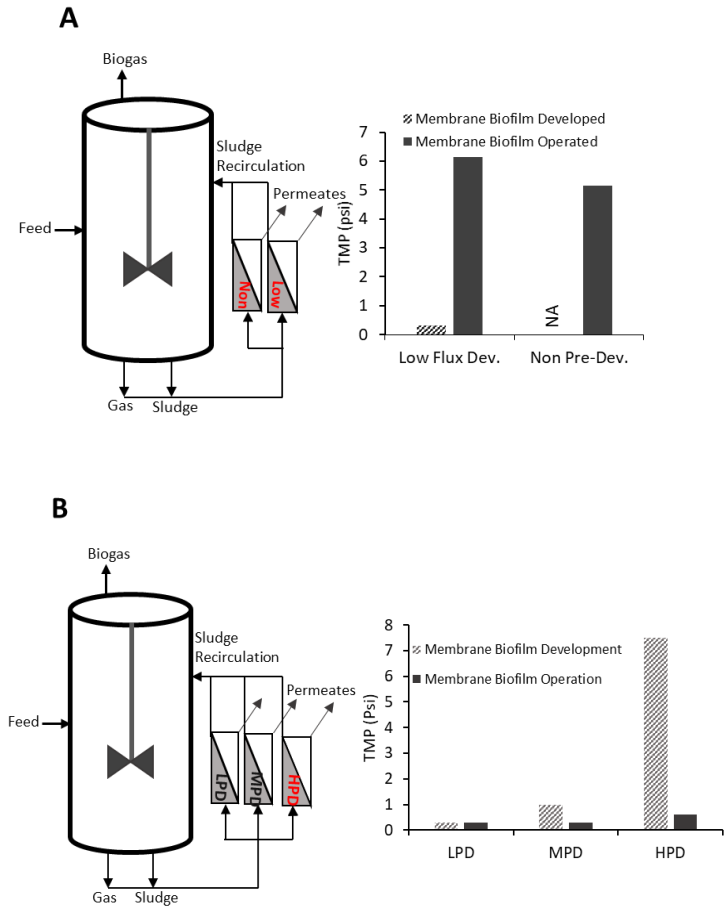

Figure 4 Schematic representations of the anaerobic membrane bioreactor operated during phases I (A) and II (B). The membrane biofilm represented in (A) was developed at low flux. In figure (B), LPD represents low flux pre-developed, MPD medium flux pre-developed, and HPD, high flux pre-development. The bar chart represents the transmembrane pressure (TMP) variations during development and operation stages of phase I and II.

4.3. Water Quality Testing

Physical and chemical water parameters of the membranes were examined by testing chemical oxygen demand (COD), total suspended solids (TSS), volatile suspended solids (VSS), and volatile fatty acids (VFAs) following standard procedures. The COD of the permeates was measured twice weekly using a Hach DR3900

Spectrophotometer following USEPA Reactor Digestion Method and colorimetric determination. Briefly, 2 mL of the sample are pipetted in sealed tubes containing dichromate and were heated in the digestor at 150 ℃ for two hours. The samples were then left to cool to room temperature, after which they were measured at 600 nm. Prior to each spectrophotometer measurement, a blank is prepared from deionized water similarly to the samples and served as the calibration blank. The COD removal was calculated as follows: $\frac{COD_{Influent} - COD_{Effluent}}{COD_{Influent}} \times 100$

Where:

COD of the influents and effluents are in mg /L.

VFAs, namely, acetate, propionate, and butyrate concentrations in the effluent samples were quantified twice weekly. The samples collected from each membrane were initially filtered using Nylon 0.2 µm syringe filters. Standards for acetate, propionate, and butyrate, were prepared in the ranges of 5 mg/L, 25 mg/L, 50 mg/L, 100 mg/L, 250 mg/L, and 500 mg/L, respectively. A standard curve was plotted for each VFA initially, with a R^2 greater than 0.95, and a representative standard was run each time to verify and calibrate the instrument. The detection was done using ion chromatography (882 Compact IC Plus) equipped with a conductivity detector and 858 Professional Sample Processor (Metrohm AG, Switzerland). The column used for the detection was a Metrosep Organic Acids - 250/7.8 (6.1005.200) column with a flow at 0.5 mL/min. The data collected are not shown because concentrations were negligible, except for one run during phase II, where the HPD membrane had lower acetate concentrations than the LPD and MPD membranes.

One of the effluent quality parameters tested was the concentration of trimethoprim, chosen to represent a wide antibiotics class because of its properties, being

hydrophilic and difficult to remove. However, the addition of trimethoprim in the influent was during phase II of the experiment at 50 µg/L. Standards were initially prepared in appropriate ranges at 10 µg/L, 50 µg/L, 100 µg/L, and 500 µg/L. Several matrices were tested for the standard curves, including ultra-pure water, influent, and effluent to ensure that the concentrations are representative. Calibration curves of the results were plotted, and results of the influent and effluent standards metrices showed equivalent concentrations as the standards prepared with ultra-pure water. The standard curves were generated and all calibration curve R^2 values were above 99%. Effluent samples collected from each membrane were prepared by filtering on a 0.2 µm Nylon filters (Whatman) using 10 mL syringes and were stored at 4 ℃ no more than 3 days prior to analysis. The preparation vials were initially washed with methanol and baked at 400 ℃ for 1 hour prior to use. The antibiotic was detected in the samples and standards and was analyzed using TSQ Endura Triple-Stage Quadrupole Mass Spectrometer (Thermofisher, USA). The LC gradient program consisted of the mobile phase A that was based on 0.1% formic acid in water and the mobile phase B that was based on 0.1 % formic acid in acetonitrile: t=0.0 min A=50% B=50%, t=3.0 min A=75% B=25%, t=5.0 min A=95% B=5%. The flow rate in the method was set at 0.3 mL/min, the maximum pressure was not allowed to exceed 600 bars, and the injection volume was 10 µL. The targeted properties of trimethoprim were as follow: molecular weight = 290.32 g/mol, retention time= 5.04 min, MS spectrum (m/z) = 291.14. The trimethoprim concentrations were calculated using matrix matched calibration curves.

4.4. Biogas and Effluent Methane Testing

The biogas production of the AnMBR was monitored daily by recording the volume and biogas content was captured in 1-L Tedlar bags and quantified by sampling the

reactor's headspace. The quantification of CH_4, CO_2, and N_2 were made by gas chromatography, Agilent 7890B, equipped with thermal conductivity detection (GC-TCD) and an oven set at 90 °C and a detector at 250 °C. Percentages of CH_4, CO_2, and N_2 were obtained from the instrument, and the methane content was normalized to CH_4 and CO_2 content by the following formula:

$$CH_4\ (\%) = \frac{CH_4(\%)}{CH_4\ (\%) + CO_2(\%)} \times 100.$$

The actual methane volume was then calculated from the biogas volume produced by the following formula: $V_{CH4} = V_{Biogas} \times \frac{CH_4}{100}$. V_{CH4} is the methane volume in L/day, V_{Biogas} is the biogas volume recorded in L/day, and CH_4 is the percentage of methane content as calculated previously.

The theoretical methane volume that is possible for an influent was calculated as follow:

$$V_{CH4\,Theoretical} = (V_{Influent} \times COD_{Influent}) \times COD_{Removal} \times Conversion\ rate_{COD\ to\ CH4}$$

Where:

$V_{CH4\,Theoretical}$ is the theoretical volume of methane expected in L/day.

$V_{Influent}$ is the influent volume fed to the AnMBR in L/day.

$COD_{Influent}$ is the COD of the influent in mg/L.

$COD_{Removal}$ is the percentage of COD removal in % as calculated previously.

$Conversion\ rate_{COD\ to\ CH4}$ is the COD to methane conversion rate of 0.25 g CH_4 / g (Appendix A). COD removed and converted to L_{CH4} / g. COD removed based on the Ideal Gas Law using:

$$Conversion\ rate_{COD\ to\ CH4} = \frac{0.25}{Mw} \times R \times T\ .$$

Where:

R is the gas constant = 0.0821 L.atm/mol.k.

T is the absolute ambient temperature in Kelvin = 298 K.

M_w is the molecular weight of methane = 16.04 g/mol.

Weekly samples for dissolved methane concentrations determination in the permeates were also measured using the headspace method. The procedure consisted of sampling 30 mL of effluent in a syringe then transfer the sample collected in the syringe to a 250 mL flask pre-filled with Nitrogen. The sample was then shaken for 1 minute, heated for 10 minutes, then shaken again briefly, which would strip the dissolved methane into the gas phase. The sample was then analyzed for methane content on GC-TCD. To evaluate the dissolved methane content, an oversaturation ratio is calculated. It follows a saturation level that is calculated based on Henry's Law constant (K_H), and the partial pressure exerted by methane in the AnMBR headspace.

The oversaturation ratio is given by: $\frac{V_{Effluent\ CH4\ calculated}}{V_{Effluent\ CH4\ Theoretical}}$

Where:

$$V_{Effluent\ CH4\ calculated}\left(\frac{mL}{L}\right) = \frac{V_{Flask\ Headspace}(mL) \times CH_4\ (\%)}{V_{Effluent\ in\ the\ flask}\ (mL)} \times 1000\ \left(\frac{mL}{L}\right)$$

$$V_{Effluent\ CH4\ Expected}\left(\frac{mL}{L}\right) = \frac{V_{CH4\ Expected\ in\ membrane\ effluent}\left(\frac{mL}{day}\right)}{V_{Membrane\ Effluent\ Collected}\left(\frac{L}{day}\right)} \times 1000$$

$$V_{CH4\ Expected\ in\ membrane\ effluent}\left(\frac{mL}{day}\right) = \frac{(K_H \times CH_{4_{Percentage\ in\ headspace}} \times 10^{-6}) \times R \times T}{M_w} \times 1000$$

Where:

K_H is Henry's Law constant, the methane solubility in water at 35 °C = 16.5 mg/L

R is the gas constant = 0.0821 L.atm/mol.k.

T is the absolute ambient temperature in Kelvin = 298 K.

M_w is the molecular weight of methane = 16.04 g/mol.

Total COD mass balance sample calculations are given in Appendix A.

4.5. Membrane Biofilm characterization

At the end of each phase, membranes were harvested and for membrane biofilm characterization, extracellular polymeric substances (EPS) were extracted. The total proteins (TP) and total carbohydrates (TC) in extracellular polymeric substances (EPS) from each membrane were quantified for both phase I and II, after membrane biofilm development stage and operation, respectively. For EPS extraction, the effective length of the membrane was cut equally spaced, into 4.75 cm x 3 cm section. The membrane biofilm was divided into two portions: the loose layer and the tight bound layer. For the loose layer on each part, the membrane surface was scraped carefully, and the biomass was suspended into a 2 mL centrifuge tube in duplicates, containing 1 mL of 1x PBS solution, and vortexed briefly at high speed. The suspension was then transferred to another falcon tube containing 5 mL of 1x PBS. For the tight layer, the same segments of membrane were further cut to equal smaller parts and added to 10 mL of 1x PBS solution, and vortexed briefly at high speed. For both the loose and tight layers, the samples were sonicated 10 times for 1 minute with 20 seconds intervals at 20 ℃ using an ultrasonic bath, UC-D10, 40 kHz (BMS, Spain). The samples were then heated for 1 hour at 100℃ and then cooled to room temperature. The samples were centrifuged at 10,000 rpm for 10 minutes. The supernatant was then transferred to a new falcon tube, the volume recorded, and the samples were stored at - 20℃.

Total carbohydrate (TC) concentration in the EPS samples was determined by the phenol-sulfuric acid method with glucose as standard adjusted (Dubois et al., 1955). Briefly, 30 µL of sample followed by 150 µL H_2SO_4 were loaded on a 96 well plate in duplicate, which was shaken briefly using a horizontal shaker or by pipetting. The plate was then incubated at 90 °C for 15 minutes. 30 µL of phenol was then added to the samples. The plate was well mixed using a horizontal shaker for 5 minutes at room temperature and the absorbance was measured using a spectrophotometer at 490 nm using SkanIt™ software for microplate readers (Thermo fisher Scientific, USA). The total proteins were quantified in duplicate by the Pierce™ BCA Protein Assay Kit, using the microplate procedure following the manufacturer's protocol (Thermo Fisher scientific, USA). The concentrations of total proteins and carbohydrates were then normalized per membrane surface are as follows:

$$TP\ or\ TC = \frac{Concentration_{Proteins\ or\ carbohydrates} \times V_{Sample\ supernatant}}{A_{membrane\ section\ cut}}$$

Where:

TP or TC are the concentrations of proteins or carbohydrates normalized to µg/cm^2.

$Concentration_{Proteins\ or\ carbohydrates}$ determined from the tests, in µg / mL.

$A_{membrane\ section\ cut}$ is the membrane area section cut during EPS extraction, in cm^2.

The biofilm layer thickness was calculated from the biomass scraped off the loose layer. The mass of a 2 mL centrifuge tube was recorded initially, then biomass sample scrapped was added to the tube. The mass of the tube and biomass was recorded. Then, the mass of the biomass layer was calculated as follows: $M_{Biomass} = M_{Biomass+tube} - M_{tube}$, where all masses were recorded in g. Then, the biofilm volume was calculated using the sludge density:

$$V_{Biofilm} = \frac{M_{Biomass}}{\rho_{Sludge}} \times 10^6$$

Where:

$V_{Biofilm}$ is the biofilm volume in cm^3.

ρ_{Sludge} is the sludge density, 970 kg/m^3.

Then, the thickness of the biofilm was calculated:

$$T_{Biofilm}\,(cm) = \frac{V_{Biofilm}(cm^3)}{A_{Membrane\ Section\ (cm^2)}} \times 10^3.$$

4.6. Microbial Community Characterization

DNA extraction was done on samples taken from the influent, effluents, suspended sludge, and membranes during phase I and II, and stored at –20 °C. Prior to storing, influent and effluent samples were filtered on 0.45 µm mixed cellulose ester (MCE) circular membrane filters (Millipore, USA). 2 mL suspended sludge was sampled weekly from the reactor, centrifuged at 12,000 rpm for 10 minutes for pellet retention which were stored at - 20°C prior to DNA extraction. During membrane harvesting at each phase of the experiment, AnMBR membrane biomass samples were taken simultaneously with EPS extraction (as described before). Membrane sections were further cut into sections of equal lengths, 4.75 x 3 cm. Biomass was scraped off the loose layer surface while the tight bound layer was further cut to smaller equal pieces, and the samples were suspended in RNAprotect Reagent (Qiagen, USA). DNA was extracted for all samples using the DNeasy PowerSoil Kit (Qiagen, USA) according to the manufacturer's protocol. Concentrations and qualities of the

extracted DNA were determined on a Nanodrop ND 1000 spectrophotometer Version 3.3.0.

Bacterial and archaeal microbial communities were characterized by amplifying the 16S rRNA gene, targeting the V4 region. Universal primers were used, 515F and 806R. Illumina NovaSeq 6000 platform was used to multiplex and sequence the PCR amplicons, was done by Novogene Genomics (Singapore), with paired-end 250 bp read lengths. Sequences obtained as FASTQ files and were analyzed on the mothur bioinformatics platform (Schloss et al. 2009) based on the Schloss Miseq SOP (Kozich et al. 2013). The sequences were filtered by the UCHIME algorithm and were aligned by the SILVA reference database (Quast et al. 2012). The sequences were then clustered into operational taxonomic units (OTUs) with an average neighbor algorithm at a 0.03 cutoff limit. Then, taxonomical classification to the genus level was done using the Ribosomal Database Project (RDP) classifier database with the 16S rRNA gene Training Set (Version 18) (Wang et al. 2007). Relative abundances were calculated based on normalization to total sequences per sample, at the genus level, and OTUs with relative abundance of 0.2 % and above were identified using the BLASTN algorithm on the National Center for biotechnology Information (NCBI) database (Altschul et al. 1990). The data obtained was used to compute Bray-Curtis similarities for phases I and II, and were visualized using the Principal Coordinate plot, an eigenvector-based approach to represent multidimensional data.

4.7. Antibiotic Resistance Gene Quantification

ARG abundances in the AnMBR effluents and membranes samples were quantified from extracted DNA samples by quantitative PCR (qPCR). Representative genes,

typically found in wastewater were selected, and were previously known to confer resistance to several antibiotic classes: class 1 integron-integrase gene (*intI1*), sulfonamides (*sul1* and *sul2*), β-lactams *(ampC* and *bla-TEM*), and tetracyclines (tetC and tetQ) (Chopra & Roberts 2001; Chen & Zhang 2013; Zhou et al. 2018). Real wastewater samples were used initially for DNA extraction to target genes by PCR and prepare qPCR standards. Targeted gel bands were excised after electrophoresis. For qPCR, the Forget-Me-Not qPCR Master Mix (Biotium, USA) was used and the samples were run on a CFX Connect Real-Time PCR Detection System (BioRad, USA). During each run, increasing temperatures from 65 to 95 °C was done, at increments of 0.5 °C, for the melt curve analysis which determined amplicon specificity. Details for the qPCR methods, primer sequences of each ARG gene targeted, thermocycling conditions, and amplicon sizes are provided in Table 1.

The standards were prepared on PCR products. The PCR reactions were conducted using 4 µL of 5x FIREPol Master Mix (Solis BioDyne, USA), 1 µL each of forward and reverse primers at 5 µM, 1 µL DNA template, and 13 µL molecular-grade water, in a 20 µL reaction. PCR products were run on a 1.5 % agarose gel and detected on a ChemiDoc Touching Imaging System (Bio-Rad Laboratories, USA). A sterile scalpel was used to excise bands, which were then purified using the GenElute Gel Extraction Kit (Sigma-Aldrich, USA) according to the manufacturer's protocol. Concentrations of gel extracts were quantified using the AccuGreen™ High Sensitivity dsDNA Quantitation Kit (Biotium) with a Qubit 2.0 Fluorometer (Thermo Fisher, USA). Thermocycling conditions for each primer set used in standard preparation are as shown in Table 2, but with the addition of a final elongation step. For qPCR, each reaction consisted of 20 µL using 10 µL of the Biotium Forget-Me-Not qPCR Master Mix, 1 µL of 5 µM each for forward and reverse primers, 1 µL of

the template, and 7 µL of molecular-grade water. Standard curves were generated during qPCR using serial dilutions of the prepared standards at 10^{-2} to 10^{-8} of the stock concentration.

Table 1 qPCR assessment details: Primers sequences, thermocycling conditions, and amplicon sizes for all genes targeted.

Gene	Primers (5'-3')	Preincubation	Amplification	Cycles	Amplicon (bp)	Reference
sul1	F- CGCACCGGAAACATCGCTGCAC R- TGAAGTTCCGCCGCAAGGCTCG	95°C for 5 min	95°C for 30 s, 55 °C for 30 s, 72°C for 60 s	40	163	(Pei et al., 2006)
sul2	F- TCCGGTGGAGGCCGGTATCTGG R- CGGGAATGCCATCTGCCTTGAG	95°C for 5 min	95°C for 15 s, 56 °C for 30 s, 72°C for 40s	40	191	(Pei et al., 2006)
tetC	F-GCGGGATATCGTCCATTCCG R-GCGTAGAGGATCCACAGGACG	95°C for 5 min	95°C for 30 s, 55 °C for 30 s, 72°C for 60s	40	207	(Naas et al., 2011)
tetQ	F- AGAATCTGCTGTTTGCCAGTG R- CGGAGTGTCAATGATATTGCA	95°C for 5 min	95°C for 30 s, 55 °C for 30 s, 72°C for 60 s	40	124	(Naas et al., 2011)
ampC	F- CCTCTTGCTCCACATTTGCT R- ACAACGTTTGCTGTGTGACG	95°C for 5 min	95°C for 45 s, 58 °C for 60 s, 72°C for 60s	40	189	(Szczepanowski et al., 2009)
bla_{TEM}	F-TTCCTGTTTTTGCTCACCCAG R-CTCAAGGATCTTACCGCTGTTG	95°C for 5 min	95°C for 45 s, 58 °C for 60 s, 72°C for 60s	40	445	(Bibbal et al., 2007)
intI1	F- CTGGATTTCGATCACGGCACG R- ACATGCGTGTAAATCATCGTCG	95°C for 5 min	95°C for 30 s, 60 °C for 60 s, 72°C for 60s	40	196	(Barlow et al., 2004)
rpoB	F- AACATCGGTTTGATCAAC R- CGTTGCATGTTGGTACCCAT	94°C for 5 min	94°C for 30 s, 50 °C for 90 s, 72°C for 90s	40	381	(Dahllöf et al., 2000)

Chapter Five

Results

5.1. Performance of the AnMBR during the experiment

The experiment consisted of two phases during which the overall performance of the AnMBR was monitored. The aim of phase I was to develop the membrane biofilm at low flux rate. The performance of the AnMBR was relatively stable during the development and operation stages of the membrane biofilms of phase I. The COD removal was in the range of 98.5 ± 0.4 % (Appendix B) and VFAs (acetate, propionate, and butyrate) were less than 10 mg/L. The TSS was in the range of 7.2 ± 0.6 g/L with an average VSS of 5.7 ± 0.2 g/L, resulting in a VSS to TSS ratio of 0.8. The methane content, increased from the development stage, 71 ± 3.3 %, to 77 ± 2.4 % during the operation stage, respectively, while the rest was attributed to carbon dioxide in the system. Figure 5A shows the methane produced compared to the expected methane values in the reactor's headspace. The average actual methane volume produced, 990 ± 0.1 mL methane / day, was close to the expected methane volume calculated, 940 ± 0.1 mL methane / day, indicating that all the COD removed was likely converted to methane.

Phase II of the experiment aimed at developing the membrane biofilm at a high flux rate, and was immediately started after phase I. The performance of the AnMBR was stable during phase II. The overall COD removal of the system was within the same range of phase I, on average 97.3 ± 1.2 %, and was consistent during the development and operation stages of the different membrane biofilms (Appendix B).

VFAs (acetate, propionate, and butyrate) were negligible throughout phase II. The only time they were detected, VFAs concentrations on the HPD membrane were lower than those found on the MPD and LPD membranes. The TSS was measured at 7.3 ± 0.5 g/L and the average VSS was 6.0 ± 0.5 g/L, resulting in a VSS to TSS ratio of 0.8. The headspace biogas produced was in accordance with the OLR of the system, and methane recovered was on average 340 mL CH4 produced / g. COD removed. The average methane content was within similar range of that of phase I, with an average of 77.2 ± 1.7 %. Figure 5B shows the methane volumes produced vs. expected in the reactor's headspace. The average actual methane volume produced, 1.1 ± 0.2 L CH_4 /day was close to the average maximum theoretical methane volume expected from COD removal, 1.1 ± 0.6 L CH_4 /day, where all the COD was most likely converted to methane (Appendix B). However, during the development stage (left side of the red line in Figure 5B), the maximum theoretical methane production was higher than the actual methane volume production. This is likely due to higher oversaturation ratios observed during the development stage.

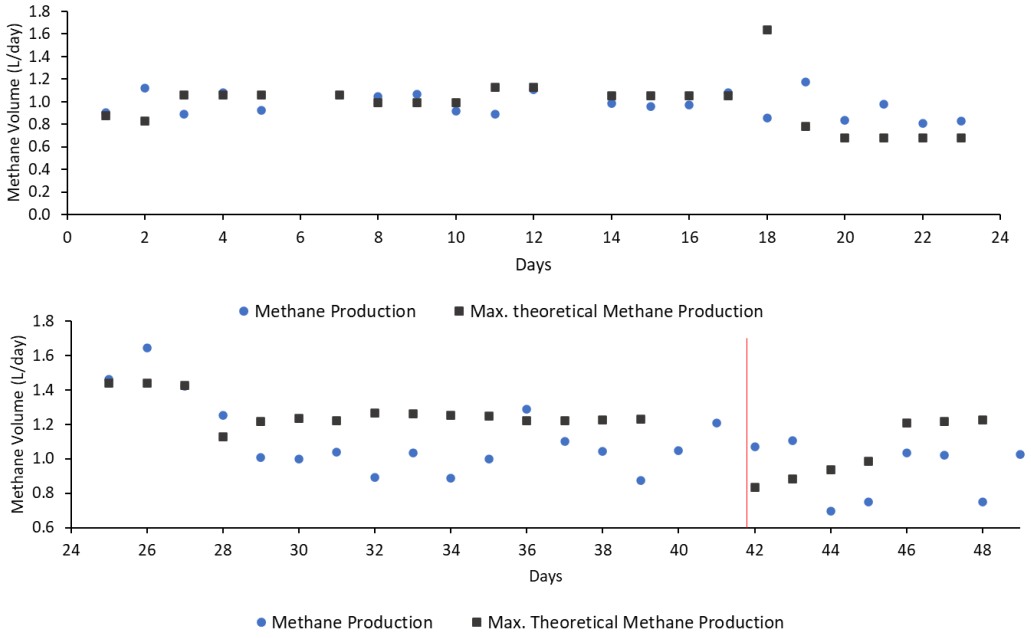

Figure 5 Methane production and maximum theoretical methane production volumes, (A) during phase I and (B) during phase II. The red line separates the development stage and the operation stage of phase II

5.2. Indifferent Performance of the Anaerobic Membrane Biofilm during Phase I

The objective of phase I was to develop a membrane biofilm at low flux rate, allowing the slow deposition of EPS and biofilm formation on the membrane surface, and thus increasing the contact between the liquid and the surface of the membrane. The low flux pre-developed membrane had a flux of 1.7 ± 0.3 L/m^2-h, resulting in a TMP of 1 psi, while another new membrane had a medium sub-critical flux of 5.2 ± 0.9 L/m^2-h, resulting in a TMP of 5.2 ± 1.0 psi. The biofilm layer was allowed to develop until a noticeable difference in biofilm layers was observed and stable TMP measures were recorded. The membrane with the low flux pre-developed biofilm layer was set to operate after at a higher flux with a new membrane without prior biofilm development, at a flux range between 4.4 and 5.9 L/m^2-h. A difference in

total membrane resistance was observed between both membranes. The low flux pre-developed membrane had a total resistance between $7.6x10^{14}$ and $8.9x10^{14}$ m^{-1}, higher than the one on the new membrane which ranged between $3.1x10^{14}$ and $4.6x10^{14}$ m^{-1} (Figure 6). In addition, permeate COD of the low-flux pre-developed membrane was relatively within same range of the new membrane, which ranged between 35 and 38 mg/L, indicating no improvements in terms of COD removal and are in agreement with the stable biogas volumes produced. Furthermore, trimethoprim was introduced at the end of phase I, in which no major difference in the permeate concentrations was observed for the low flux pre-developed membrane biofilm compared to a new one, with value on average of 11.7 ± 1.3 µg / L and 12.6 ± 3.5 µg /L, respectively.

The total proteins (TP) to total carbohydrates (TC) ratios varied greatly between the tight and loose layers during development and operation stages for the low flux pre-developed biofilm membrane. TP / TC ratio of the tight layer at the end of the development stage was found to be 4.67 while the loose layer wasn't recovered (Figure 7A). However, the operation of the membrane at higher TMP resulted in a higher TP/TC ratio in the tight layer, and also in the presence of the loose layer, being at the same range of the tight layer, at 5.03 and 5.06, respectively (Figure 7B). The thickness of the loose layer of the membrane biofilm pre-developed at low flux was found to be 31.25 µm compared to the thickness of a new membrane of 10.71 µm (Table 2). Overall, these results indicated that the biofilm pre-developed at low pressure didn't contribute to a better permeate quality but resulted in an increase in TMP. Thus, another strategy, represented by phase II, was devised to investigate the effect of developing a membrane biofilm at high pressure.

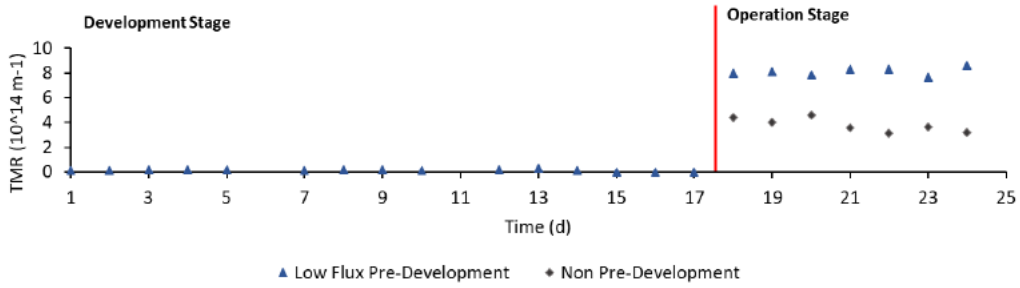

Figure 6 Total membrane resistance (TMR) during the development and operation stages of the membrane biofilms in the AnMBR, for phase I.

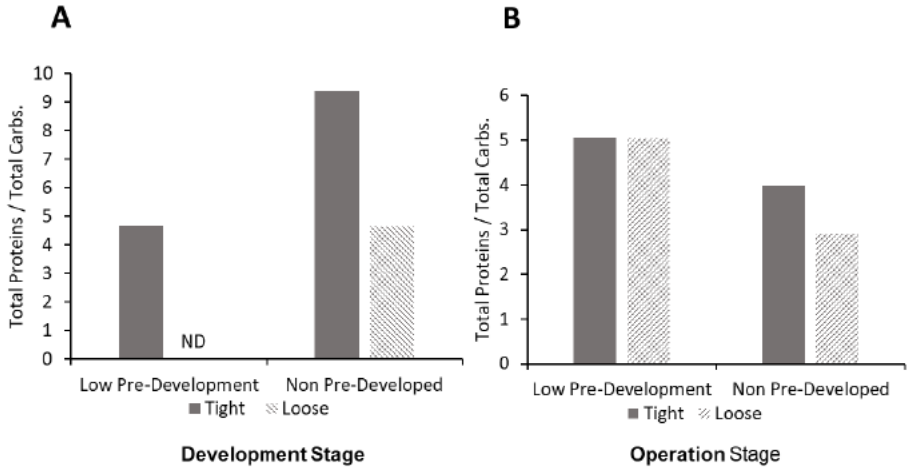

Figure 7 Total proteins to total carbohydrates ratio during the development stage (A) and operation stage (B) of phase I for the membranes (tight and loose layers) in the AnMBR. ND indicates not detected.

Table 2 Membranes biofilm thickness calculations during phases I and II.

Membrane	M_{tube} (g)	$M_{Biomass+tube}$ (g)	$M_{Biomass}$ (g)	$V_{Biofilm}$ (cm^3)	$A_{Mem\ Section}$ (cm^2)	$T_{Biofilm}$ (µm)
Low-Flux Pre-Dev.	1.03	1.07	0.04	0.04	14.25	31.25
Non-Pre-Dev.	1.05	1.06	0.01	0.02	14.25	10.70
LPD	0.95	0.97	0.01	0.01	9.50	14.11
HPD	1.63	1.66	0.02	0.02	9.5	26.26

5.3. Distinct Characteristics of the Anaerobic Membrane Biofilm during Phase II

5.3.1. Transmembrane Pressure and Biofilm Sustainability

The objective of phase II was to investigate the effect of membrane biofilm formation at high pressure on the effluent quality. Thus, the membranes from phase I were harvested and replaced by three membranes, on which biofilms were allowed to develop simultaneously. The LPD membrane biofilm was developed at a flux of 3.9 ± 0.2 L/m^2-h, the MPD membrane biofilm at 6.9 ± 0.3 L/m^2-h, and the HPD membrane biofilm at 7.0 ± 0.4 L/m^2-h, which resulted in TMPs of 0.3 psi, 1.0 psi, and 7.5 psi, respectively. It is noteworthy that the pumping rate set for the HPD membrane resulted in a supercritical flux, leading to immediate fouling and reduction of the flux to 7.0 ± 0.4 L/m^2-h. After biofilm development was noticeable by monitoring visually the biofilm layer and the stability of TMP, at day 41, the membranes were set at the same flux rates ranging between 3.9 and 5.4 L/m^2-h to compare the effect of the biofilm on the membranes performance. TMR profiles were plotted, and values obtained were closer in this phase than they were in phase I. When comparing the three membranes, TMR values ranged between 0.3 and 0.7 10^{14} m^{-1}(Figure 8). The results suggest that the membrane biofilm originally developed at high TMP was able to rapidly adapt and maintain very low TMPs thereafter, over the operation time of the study. In fact, membrane resistance, indicated by TMR values, has been attributed previously to fouling mechanisms, and different fouling modes include pore blockage, cake formation, and intermediate or complete pore blockage (Charfi et al., 2012).

To investigate the TMR profiles in relation with biofilms developed, EPS extractions were characterized for total proteins and total carbohydrates content for each membrane and are shown in Figure 9. It is noticeable that the total proteins concentrations are higher for all membranes, which is consistent with previous studies (Xiong et al., 2016; Chen at al., 2017; Cheng et al., 2021; Xu et al., 2022). However, the total proteins to total carbohydrates ratio was only consistent for the HPD membrane during the operation stage on both the tight and loose layers, with ratios of 9.0 and 9.1, respectively. A similar trend was observed during the operation stage of the pre-developed membrane biofilm in phase I, during which the tight and loose layers were found to have a consistent total protein to total carbohydrates ratio, even with higher TMR values observed. Although adhesion forces were correlated with EPS (namely proteins) and hydrophobic membranes (such as PVDF) at higher OLRs (Chen at al., 2017), the observations in this study could explain a dissociation between TMP and biofilm inhibition. Contrary to what has been previously reported for the effect of membrane material on fouling, the observations in this study showed that the membrane material is not necessarily the key component for biofilm attachment since the three membranes materials used were identical. However, it remains an important aspect for initial adhesion on the membrane surface. In addition, the thickness of the loose layer of the HPD membrane biofilm was estimated at 26.3 μm, which is greater than that of the LPD, at 14.1 μm (Table 2). Combining the fact that the HPD membrane's TMP was recovered during the operation stage, EPS content had higher total proteins concentrations, and a thicker layer, it is likely that least partial pore blocking occurred, but instead a biocake layer was developed and maintained on the HPD membrane.

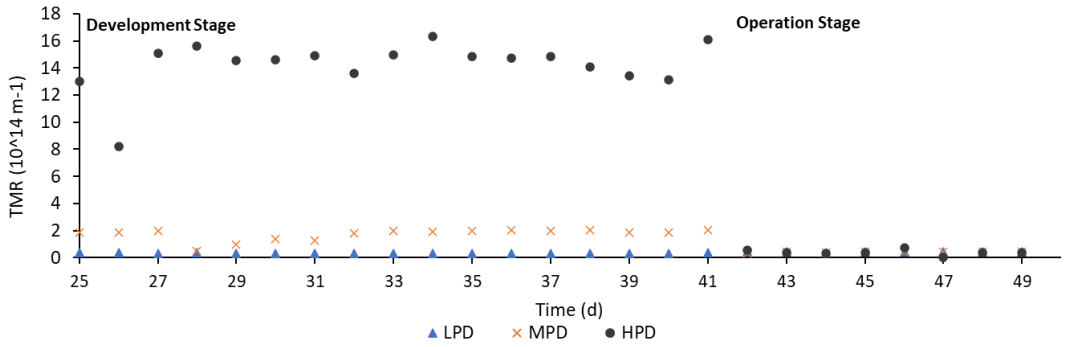

Figure 8 Total membrane resistance (TMR) during the development and operation stages of the membrane biofilms in the AnMBR, for phase II. LPD represents the biofilm pre-developed at low pressure, MPD represents the biofilm pre-developed at medium pressure, and HPD represents the biofilm pre-developed at high pressure.

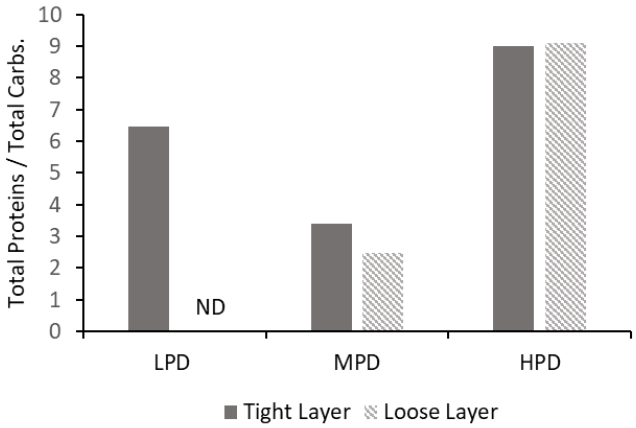

Figure 9 Total proteins to total carbohydrates ratio during the operation stage of phase II for the three membranes (tight and loose layers) in the AnMBR. ND indicates not detected. LPD represents the biofilm pre-developed at low pressure, MPD represents the biofilm pre-developed at medium pressure, and HPD represents the biofilm pre-developed at high pressure.

5.3.2. Antibiotics Removal

To investigate the effect of membrane biofilm on the removal of emerging contaminants, trimethoprim was chosen to represent a major antibiotic class found in wastewater because of its hydrophobic properties and was added to the influent at 50 µg/L of phase II. Results in Figure 10 shows that during the development stage of the

HPD membrane, the trimethoprim permeate concentrations on all membranes had an average value between 26.7 µg/L to 28.7 µg/L, and the concentrations were consistently higest during the biofilm development stage. However, during operation stage, the HPD membrane showed lowest trimethoprim concentration, 20.28 ± 5.70 µg/L, with the concentrations of the HPD having the lowest values consistently (Figures 10 & 11).

Removal of trimethoprim in anaerobic mainstream treatment varied in previous studies, however, biodegradation was the main removal mechanism. Previous studies found that trimethoprim belongs to electron-donating groups and reported low sludge sorption susceptibility with a relatively low partitioning coefficient (K_d), at $K_d < 3.2$ (Monsalvo et al., 2014). For removal comparison among the three membranes with previous studies, a pseudo-first order kinetic model was applied to the bioreactor membranes with a reaction rate defined as:

$$r = -k_{BD}.X_{VS}.C$$

Where the biological degradation constant is represented by k_{BD} (L / gMLVSS.d), X_{VS} is the concentration of mixed liquor volatile suspended solids, MLVSS,(g/L), and C is defined as the concentration of trimethoprim in the reactor (µg/L). This model considers operational parameters that affect biological removal rates such as MLVSS that represent biomass concentrations and HRT. Based on the removal rate of each membrane, k_{BD} values were calculated for both development and operational stages and are presented in table 3. During the development stage, the removal rates for LPD, MPD, and HPD membranes were found to be very close, resulting in highly similar K_{BD} values (0.15 L / gMLVSS-d). On the other hand, during operation stage, HPD membrane showed highest K_{BD} value of 0.18 L/ gMLVSS-d while LPD and MPD values were 0.054 L/ gVSS.d and 0.099 L/ gVSS.d, respectively. A recent

study on emerging contaminants removal in a UASB which applied a pseudo-first order kinetic model would result in a K_{BD} of 0.14 L/ gMLVSS-d, a value similar in range to the one found in our study (Monsalvo et al., 2014).

Due to its low sorption capacity, biodegradation was previously reported as the main pathway for trimethoprim removal during anaerobic digestion. Among the degradation processes of trimethoprim are transformation through demethylation and via ether cleavage. The biodegradation of trimethoprim was also coupled with sulfate respiration and methanogenic activity (Ghattas et al., 2017; Harb et al., 2017; Liang et al., 2019). More interestingly, the highest K_{BD} value corresponded with the highest removal rate observed on the HPD membrane with the highest loose layer thickness. Contrarily to results in phase I in which trimethoprim concentrations in the permeate were within the same range for both the low flux pre-developed membrane and the new membrane, the observations from phase II suggested that the HPD membrane biofilm contributed directly to the biodegradation of the antibiotic.

Table 3 Trimethoprim influent and effluent concentrations, removal rates, and K_{BD} values during phase II.

	Development Stage			**Operation Stage**		
	LPD	MPD	HPD	LPD	MPD	HPD
Inf. Conc. (µg/L)		52.0 ± 6.1			51.8 ±3.0	
Eff. Conc. (µg/L)	24.6 ± 9.7	25.6 ± 9.0	26.1 ± 9.4	34.5 ± 10.4	27.5 ± 5.8	20.3 ± 5.7
Removal Rate (%)	53.3	53.6	53.2	32.5	47.0	61.4
K_{BD} (L/ g.VSS-1.d-1)	0.15	0.15	0.15	0.05	0.10	0.18

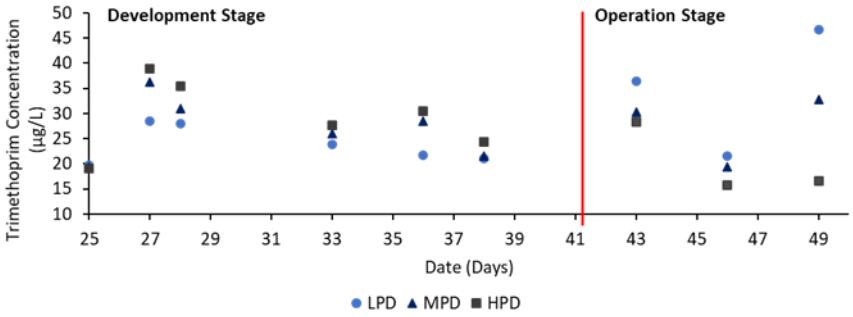

Figure 11 Trimethoprim concentration average values in the AnMBR effluents during both development and operation stages for the three membranes studied (phase II).

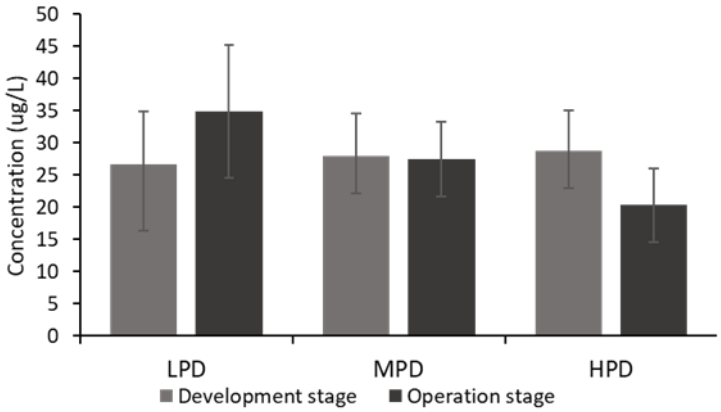

Figure 10 Trimethoprim effluent concentration variations at different membrane biofilm flux during development and operation stages of the experiment (Phase II). Influent trimethoprim concentration = 50 µg/L.

5.3.3. COD Removal and Dissolved Methane Concentration

The membrane biofilms pre-development strategies seemed to have different effects on COD removal and dissolved methane concentrations during the operation stage, specifically for the HPD membrane. During the development stage, the HPD membrane showed consistently the lowest COD concentration, with an average of 26 ± 10.6 mg / L, while LPD and MPD, had average values of 68 ± 60.6 mg/L and 50 ± 10.6 mg/L, respectively. The high standard deviations calculated are due to variations in COD values measured during the experiment but were consistent within each

other. The HPD membrane also resulted in the lowest permeate COD, which was consistently lower during the operation stage of the experiment, with a COD value on average of 13.7 ± 9.6 mg/L, while LPD and MPD membranes COD permeate values were in the same range, 21.3 ± 9.5 and 21 ± 11.1 mg/L, respectively (Figure 12). The dissolved methane content in the effluent, however, showed contrary results during both development and operation stages, in which the HPD membrane oversaturation ratio was always higher. It was observed that from days 25 to day 50 of phase II, during the development stage, the oversaturation ratios in LPD, MPD, and HPD membranes permeates were on average 1.04 ± 0.14, 1.11 ± 0.22, and 2.31 ± 0.41, respectively. A previous study recorded similar ranges for membranes operated at similar TMPs (Smith et al., 2014). When membranes were operated at similar flux rates, the oversaturation ratios decreased for all membranes, but the HPD membrane remained the highest, at 1.02 ± 0.09, and LPD and MPD, 0.82 ± 0.05 and 0.87 ± 0.2, respectively (Appendix B).

Furthermore, it is noticeable that the high TMP on the HPD membrane resulted in higher oversaturation ratio and dissolved methane in the permeate following higher COD removal. Furthermore, since stable operation was observed for the AnMBR, COD removal and higher dissolved methane content in the permeate was attributed to the biofilm developed on the HPD membrane. Further studies testing the membrane materials effects on the permeability are required. Nonetheless, the current study showed that the effects of the high TMP biofilm development could be extended beyond the development stage and can be observed at lower TMP. This effect was not found to hinder the performance of the AnMBR, since the total membrane resistance decreased at lower TMP during the operation stage.

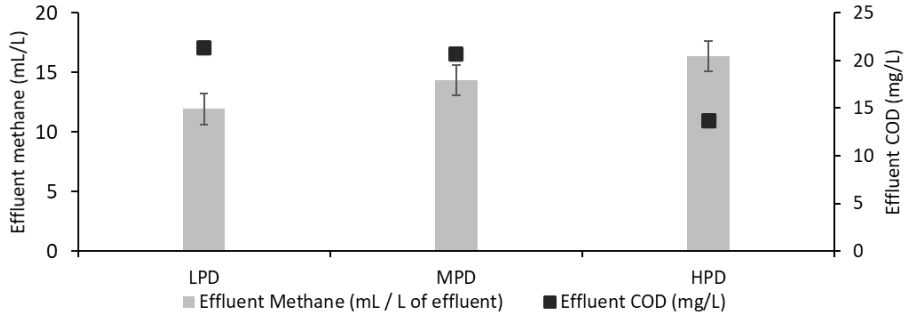

Figure 12 Effluent methane and COD average values of the AnMBR throughout phase II. The bars represent standard deviations. LPD represents low pre-developed membrane biofilm, MPD, medium pre-developed membrane biofilm, and HPD, high pre-developed membrane biofilm.

5.4. Microbial Communities Profiles in the AnMBRs Samples

5.4.1. Microbial Communities Differences between phases I and II

The microbial communities' dynamics at the different devised biofilm development strategies was found to vary throughout the experiment. Principal coordinates analysis (PCoA) plots of microbial abundance using Bray Curtis distance matrix at genus level clustering during phases I and II was used for analysis. In particular, divergence in microbial communities during phase II in the sludge and membrane samples based on PC2, indicated a clear difference between membrane biofilm and sludge microbial groups, except for the loose membrane layers, which showed high similarity between LPD and HPD membranes regardless of development strategy (Figure 13). The microbial abundance of the tight layer of a new membrane was also shown to be highly different than others from the sludge and biofilm samples. These observations are in accordance with a previous study that analyzed the differences between membrane biofilm and sludge communities and reported dissimilarity between MBR sludge samples and biofilm samples, and more specifically, early, and mature biofilm samples (Matar et al., 2017). The divergence in microbial abundance during phase II is unlikely to be explained by random assembly, but rather the result

of unique OTUs that were favored under the devised biofilm strategies. This observation is further highlighted in the PCoA plot of microbial abundance using Bray Curtis similarity distance matrix for genus level clustering during phase II. While AnMBR sludge and effluent samples showed dissimilarity based on PC1 (59.4 %), the HPD membrane tight layer was clearly distinct from all other samples, based on PC2 (11.4%). On the same note, a previous study conducted by Harb et al. (2015), on two-lab scale AnMBR, one continuously stirred (CSTR) and one up-flow attached growth (UA), treating synthetic municipal wastewater, showed that despite initial similarity between sludge and biofilm microbial communities in CSTR and the UA reactors, complete division was observed even under the same operating conditions.

Results in Figure 14 show the relative abundances (RA) of microbial communities of the AnMBR membrane samples at the end of phases I and II, with RA greater or equal to 0.4 in at least one sample. It is noteworthy to state that the LPD membrane and non-pre-developed membrane were subjected to the same operating conditions, as stated previously. A comparison between the tight and loose layers of the membranes revealed that the tight layers were more different than the loose layers, except for genera related to *unclassified Pseudomonadaceae* and *Methanocospusculum,* that were found higher on the loose layer of the non pre-developed membrane. Furthermore, for the tight layers, the HPD membrane was clearly different than the tight layers of the LPD and non pre-developed membranes and among the main differences on the HPD membrane were genera related to *unclassified Rhodocyclaceae* with RA 18%, *Acinetobacter* with RA 6.8%, and *Acidovorax* with RA 2.6 %. Genera related to *Fervidobacterium, unclassified Comamonadeceae, unclassified Anaerolineaceae, Desulfovibrio,* and *Dechloromonas,* were found at similar RAs on the tight layers of the LPD and non-

predeveloped membrane biofilms. Considering further the higher performance attributed to the HPD membrane in terms of better effluent quality, the biofilm layer developed at high TMP resulted in unique taxa that conferred advantages to the HPD membrane when compared to the others. These results contribute to the understanding of the interaction between microbial communities' dynamics under different AnMBR operating conditions and their influence on the performance, specifically on the membrane performance. Core sludge microorganisms were previously reported to be present in the AnMBR regardless of the operating conditions and would eventually become the main source of microorganisms for the membrane biofilm. Moreover, it has been described that the microbial composition on the membrane could be assembled through random migration, following a neutral assembly model (cheng et al., 2019. The PCoA comparing microbial abundances between phases I and II (Figure 15) showed that the AnMBR microbial communities were found to be closely clustered based on the secondary principal coordinate (PC2, 38.2 %) during phase I while being significantly separated during phase II based on the primary principal coordinate (PC1, 27.4 %). These results could explain the effect of TMP on the membrane dynamics during phase II, in which selected microbial groups were favored. Furthermore, these finding highlight the positive interaction between abiotic and biotic parameters that influence the biofilm's formation and subsequently its activity.

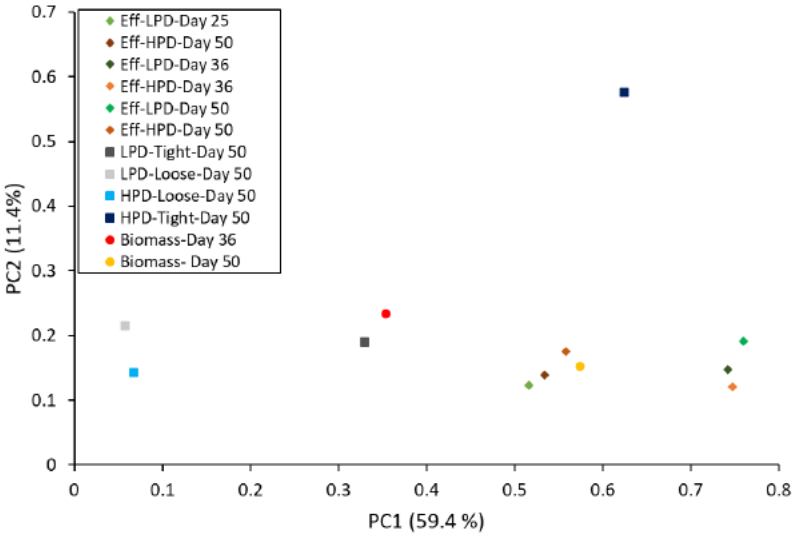

Figure 14 Principal coordinates analysis (PCoA) plot of microbial abundance showing similarity using Bray Curtis similarity distance matrix for genus-level clustering for phase II. LPD represents the biofilm pre-developed at low pressure, MPD represents the biofilm pre-developed at medium pressure, and HPD represents the biofilm pre-developed at high pressure.

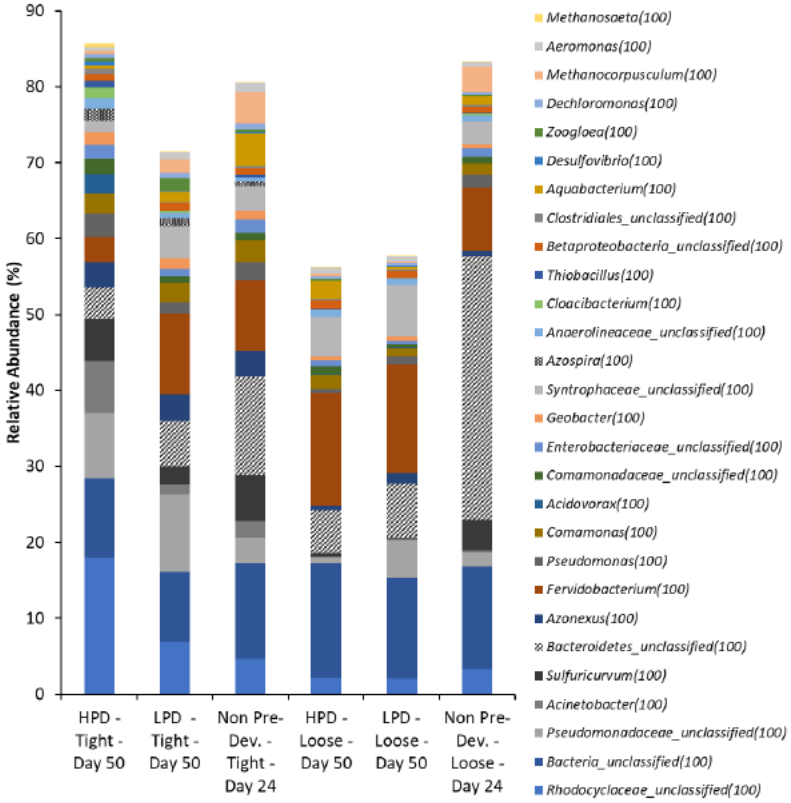

Figure 13 Relative abundance of microbial community operational taxonomic units at the genus level in the loose and tight membrane layers at the end of Phases I and II, with RA greater than 0.4% in at least one sample. HPD represents highly pre-developed biofilm layer and LPD represents low pre-developed biofilm layer.

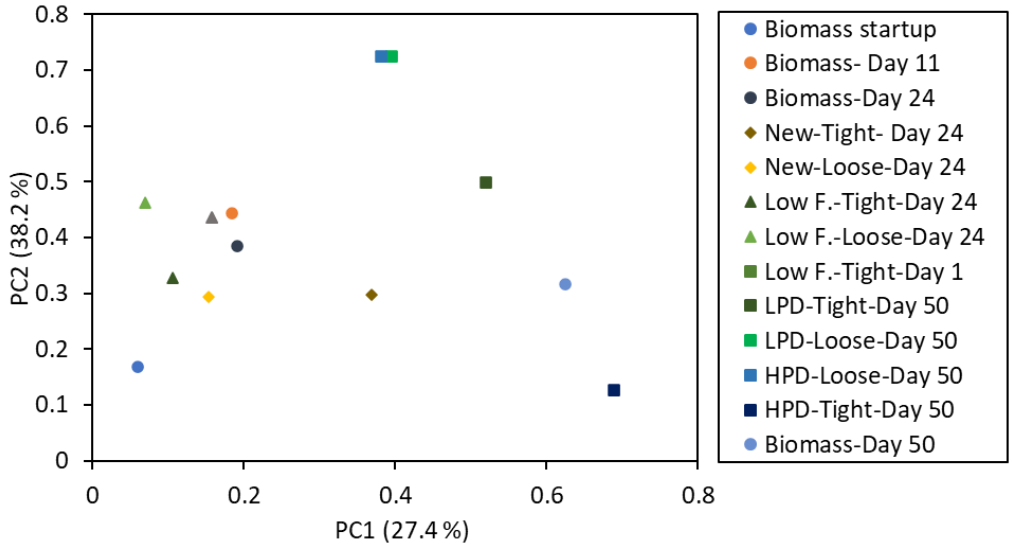

Figure 15 Principal coordinates analysis (PCoA) plot of microbial abundance showing similarity for AnMBR samples using Bray Curtis similarity distance matrix for genus-level clustering for phases I and II. New represents a new membrane, Low F represents the membrane biofilm pre-developed at low pressure, and biomass represents the reactor's sludge. Tight and loose are the membrane layers for each sample. Day 24 marks the end of phase I while Day 50 is the end of the experiment.

5.4.2. Selective Microbial Groups on the Tight Layer of the HPD Membrane

The predevelopment of the membrane biofilm at high TMP initially, resulted in unique OTUs. Results in Figure 16 highlight the relative abundances (RA) of genera that were found the most abundant on the tight layer of the HPD membrane. The relative abundance of phyla related to *Proteobacteria, Campilobacteria, Thermotogae, Spirochaetes, Chloroflexi,* and *Firmicutes* represented 62.5 % of the total relative abundance on the tight layer of the HPD membrane while these phyla accounted for 33% of the tight layer of the LPD membrane. As previously stated, the relative abundances of the microbial communities on the loose layers of the HPD and LPD membranes were closer to each other than that of the tight layers, but with lower RA, of 28.5 % and 25.8 %, respectively. Even at lower RA, between 0.1 % and 1%, the HPD membrane tight layer was found to possess distinct microbial groups (Figure 16B). More interestingly, the genera found with the highest relative

abundance on the HPD membrane were groups identified as capable of fermentation and thus contributing to anaerobic digestion, biodegradation of emerging contaminants of concern, and others known to enhance methanogenic activity via the presence of syntrophic relations (Zarei-Baygi et al., 2020; Saia et al., 2016).

Among the fermentative groups, genera related to *Azonexaceae* (12.9%), *Pseudomonadaceae (*7.7 %), *Acinetobacter* (6.9 %), *Azospira* (1.6 %), and *Clostridiales* (0.5 %), showed highest RA on the HPD membrane tight layer. Those microorganisms were among groups previously identified as core microbial microorganisms in anaerobic digestion, having key role in the degradation and metabolism of several monomers, xenobiotics, and organic compounds (Amin et al., 2021; Weiß et al., 2013; Wu et al., 2016; Wang et al., 2019; Fujimoto et al., 2019). Similarly, unclassified *Anaerolineaceae* (1.4 %), *Desulfovibrio* (0.5 %), *Sulfuricurvum* (5.5 %), and *Thiobacillus* (0.9 %) were found to be the highest on the tight layer of the HPD membrane and have been reported to play key role in the biodegradation of compounds containing aromatic rings and more specifically, trimethoprim (Vigneron, 2017; Liang et al., 2019). The biofilm developed on the HPD membrane and specifically on the tight layer was favorable for selected groups growth capable of transforming trimethoprim. In their study, Liang et al. (2019) also reported the acclimation of such consortia capable of trimethoprim removal through demethylation. They also observed that anaerobic biodegradation of trimethoprim could be coupled with sulfate respiration, in which sulfate is the electron acceptor. In their study, Jia et al. (2019) examined the removal of eight pharmaceuticals in an anaerobic sulfate-reducing bacteria (SRB) sludge system, of which was trimethoprim. They reported in their results that among the main functional enzymes

found in the SRB sludge, cytochrome P450 (CYP450) was responsible with trimethoprim removal (Jia et al., 2019).

Indeed, the biofilm developed in phase II harbored sulfur-reducing (microorganisms capable of reducing elemental sulfur to hydrogen sulfide) and sulfur-oxidizing bacteria (microorganisms capable of sulfur-driven denitrification). Among these, *Sulfuricurvum Kujiense*, detected with highest RA of 5.46% on the HPD membrane, and belonging to the *Sulfuricurvum* genus, is known to grow anaerobically in the presence of sulfide or thiosulfate as electron donors, and nitrate as an electron acceptor, and produce extracellular elemental sulfur particles. Furthermore, certain *Thiobacillus spp.*, such as *Thiobacillus sajanensis* (Table 4), also detected with highest RA on the HPD membrane (0.94 %), are capable of denitrification utilizing sulfide. Sulfide is commonly found in the form of hydrogen sulfide, a toxic contaminant of biogas produced during anaerobic digestion. Genera related to *Thiobacillus* eventually convert sulfide to elemental sulfur or sulfate. It has been proven that *Thiobacillus* genera are activated by the small supply of air (micro-aeration) while they grow in a microaerophilic environment on CO_2 (Kiran et al., 2016). In fact, microaeration has been recently describes as an effective approach to enhance anaerobic digestion trough hydrolysis acceleration, hydrogen sulfide removal, prevention of VFAs accumulation, and ultimately increased methane production (Chen et al., 2020). Thus, the anaerobic biofilm developed is not only related to increased removal of contaminants, but also could confer advantages in terms of biogas quality enhancement.

The tight layer of the HPD membrane was also found to have advantageous membrane biofilm activity because of selected genera that could enhance methanogenic activity. Furthermore, analysis of the microbial communities at the

family level was done to compare the relative abundance of microbial groups in the suspended sludge of the bioreactor with the membrane and effluent samples (Figure 17). Results showed great discrepancy between all membrane samples and the biomass, namely the tight layer of the HPD membrane. To elucidate further the difference attributed to the HPD membrane, a subsequent analysis of microbial communities was done on the genus level. Highest RA for genera related to *Methanosaeta* (0.4 %), *Methanospirillum* (0.2 %), *Fervidobacterium* (3.3 %), *Acidovorax* (2.6 %), *Rectinema* (1.6 %), *Geobacter* (1.6 %), and *Syntrophomonas* (0.3 %) are highlighted (Figure 16A and 16B). *Methanobacterium* RA was also highest on the HPD membrane (0.085%), although not shown in the figures. However, methanogens such as *Methanocorpusculum* and *Methanomassiliicoccus* were found to have highest RA on the tight layer of the LPD membrane. The methanogenic activity during anaerobic digestion should not be overlooked for its role in methane production as well as the degradation of various aromatic micropollutants, in addition to syntrophic capacity (Ghattas et al., 2017). In particular, the average biotransformation efficiencies of sulfamethoxazole and trimethoprim showed higher efficiencies during methanogenesis (Gonzalez-Gil et al., 2018). Similar results to ones found here were reported by Aziz et al. (2022), who found higher elimination of sulfamethoxazole, trimethoprim, and naproxen during anaerobic digestion in relation with *Methanothrix spp.* The methanogens enriched on the biofilm were previously observed to have relations with *Geobacter*, a core bacterium known to be exoelectrogenic, and *Syntrophomonas*, because of their affinity for membrane biofilms (Harb et al., 2015). It is not the first time that anaerobic membrane biofilms are reported to have increased antibiotic degradation over the suspended biomass (Harb et al., 2021). Furthermore, recent studies found

that some of the genera mentioned above play a role in enhancing bio-methanization, which was observed exclusively on the HPD membrane. Among those genera, *Rectinema,* known for sulfate reduction and fermentation capabilities, was proven present in methane generating consortia such as *Methanothrix*,,and *Acidovorax,* was reported as is capable of biochemical conversions of CO_2 to CH_4 (Kabaivanova et al., 2022; Dong et al., 2022). A recent study treating *Scenedesmus* microalgae in an AnMBR, suggested relevant methane producing pathways dependent on fermentative microbes such as *Anerolineaceae,* which was enhanced through the biofouling development in the membrane tank (Zamorano-López et al., 2019). Overall, the conditions under which the membrane biofilm was developed, i.e at high TMP initially, proved advantageous during its operation, specifically on the tight layer of the membrane, where selective microbial groups were enriched and were maintained throughout the operation phase.

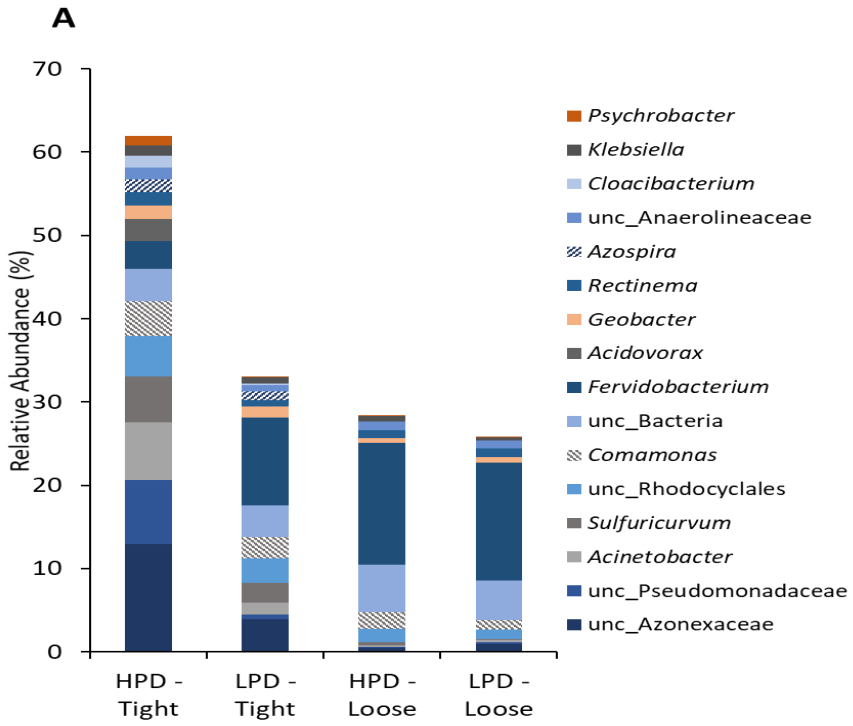

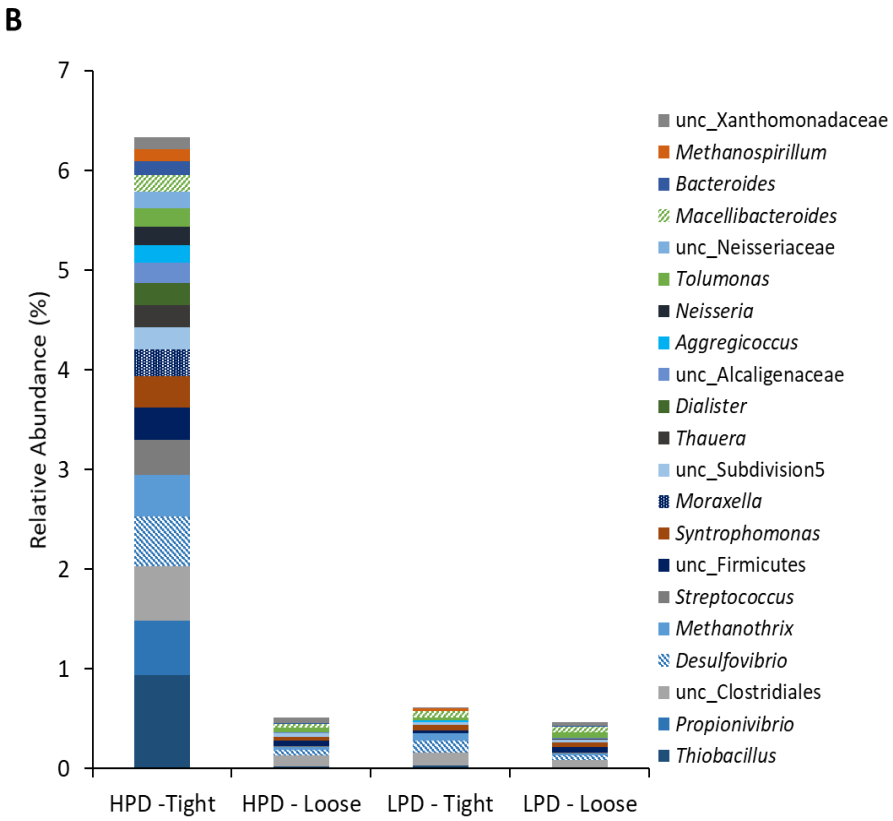

Figure 16 Relative abundance, RA, (%) of microbial community operational taxonomic units (OTUs) at the genus level in the loose and tight membrane layers of the AnMBR samples at the end of Phase II with the highest relative abundance on the HPD-tight membrane with (A) RA greater than 1% and (B) RA between 0.1 % and 1%, respectively. HPD represents highly pre-developed biofilm layer and LPD represents low pre-developed biofilm layer.

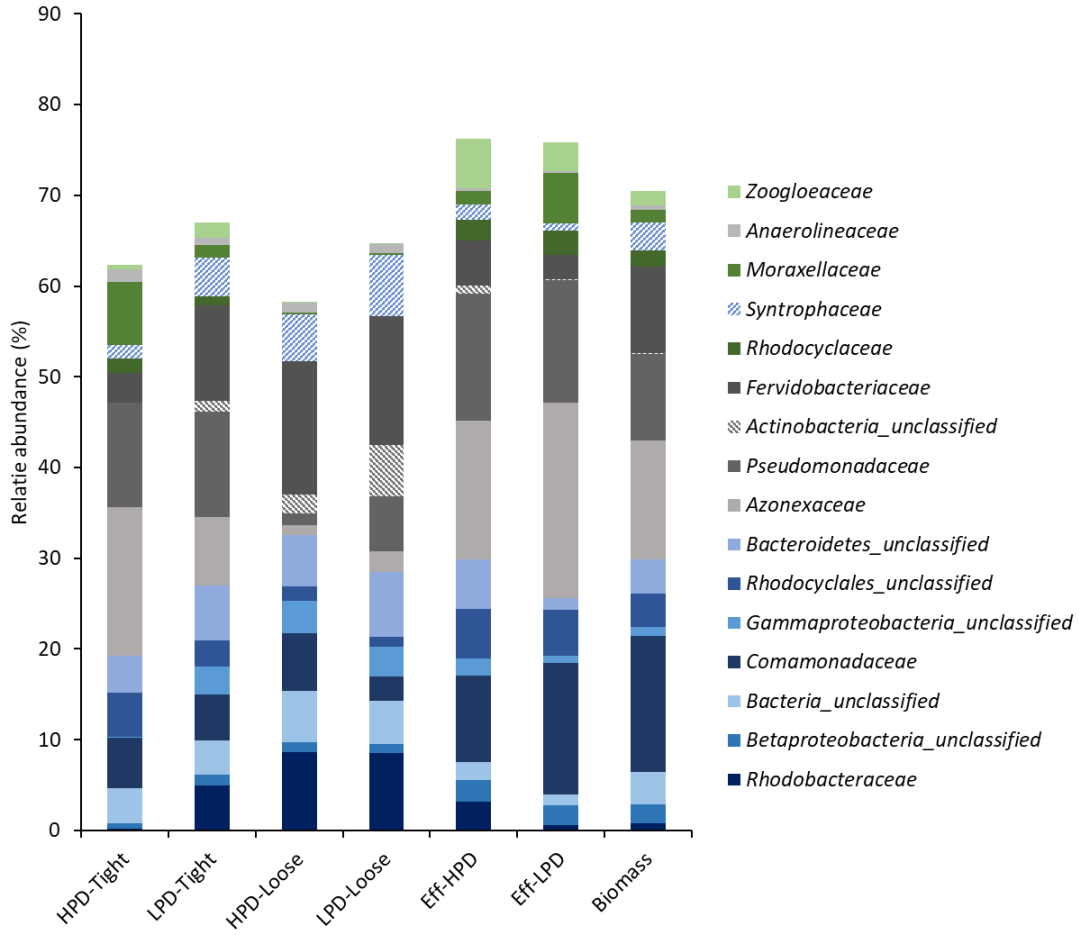

Figure 17 Relative abundance, RA (%), of microbial community operational taxonomic units (OTUs) at the family level at the end of phase II, with RA greater than 2% in at least one sample. Tight and loose represent the tight and loose layers of the membrane samples. HPD represents highly pre-developed biofilm layer and LPD represents low pre-developed biofilm layer. The biomass was sampled from the reactor's sludge.

Table 4 Representative species of nearest sequence similarity, with the relative abundance (RA) highest on the HPD membrane tight layer. LPD and HPD represent the low predeveloped and high predeveloped membrane biofilms, respectively. Loose and tight represent the layers of each membrane biofilm.

Species	LPD - Loose	HPD - Loose	LPD - Tight	HPD - Tight
Azovibrio restrictus (100%)	0.96	0.50	3.94	12.96
Acinetobacter dispersus/ tandoii/ tjernbergiae/haemolyticus/ parvus/ beijerinckii (100%)	0.24	0.22	1.39	6.91
Diaphorobacter polyhydroxybutyrativorans/nitroreducens; Ottowia beijingensis/shaoguanensis/pentelensis ; Comamonas faecalis/serinivorans; Brachymonas chironomi (100%)	1.15	1.99	2.63	4.22
Azospira restricta (97.08%)	1.09	1.62	2.88	4.85
Pseudomonas resinovorans/ guangdongensis (99.6%) or Pseudomonas aeruginosa /otitidis /oryzae/ guezennei (99.21 %)	0.21	0.03	0.57	7.70
Sulfuricurvum kujiense (99.21%)	0.16	0.41	2.40	5.46
Azospira oryzae (100%)	0.01	0.01	1.04	1.56
Acidovorax temperans/defluvii (100%)	0.00	0.01	0.01	2.64
Geobacter lovleyi SZ/thiogenes (100%)	0.64	0.53	1.35	1.64
Rectinema cohabitans (94.86 %)	1.00	0.96	0.76	1.60
Leptolinea tardivitalis (91.67%)	0.95	1.03	0.76	1.43
Klebsiella / Enterobacter / Salmonella species (1005)	0.37	0.71	0.72	1.28
Cloacibacterium normanense/ rupense/ caeni/rupense (100%)	0.00	0.00	0.23	1.35
Psychrobacter sanguinis (100%)	0.01	0.00	0.00	1.17
Thiobacillus sajanensis (100%)	0.01	0.03	0.03	0.94
Moraxella osloensis (1005)	0.00	0.01	0.00	0.63
Aliarcobacter lanthieri/cibarius/ cryaerophilus (99.60%)	0.00	0.00	0.00	0.56
Propionivibrio limicola (98.81 %)	0.00	0.00	0.00	0.55
Clostridium oceanicum (91.73%)	0.08	0.11	0.13	0.55
Desulfovibrio mexicanus (99.60%)	0.05	0.05	0.12	0.50
Novispirillum itersonii species (100%)	0.00	0.00	0.00	0.48
Ruminiclostridium cellobioparum subsp. termitidis /Acetivibrio alkalicellulosi (92.89%)	0.38	0.38	0.38	0.47
Methanothrix/ Methanothrix soehngenii (100%)	0.02	0.03	0.07	0.41
Pseudescherichia vulneris/shigella species / Escherichia species (100%)	0.00	0.00	0.00	0.37
Streptococcus minor (99.60%)	0.00	0.01	0.00	0.36
Phascolarctobacterium faecium (85.04%)	0.05	0.05	0.03	0.32
Syntrophomonas zehnderi OL-4 (97.65%)	0.05	0.04	0.06	0.32
Anaerosinus glycerini (100%)	0.02	0.02	0.09	0.18
Actinobacillus seminis (98.81 %)	0.00	0.00	0.00	0.28
Moraxella cuniculi (99.60 %)	0.00	0.00	0.00	0.26
Labilibacter marinus (90.94%)	0.10	0.07	0.02	0.25
Castellaniella caeni / daejeonensis / defragrans / ginsengisoli (100%)	0.00	0.00	0.03	0.04
Luteitalea pratensis (82.75 %)	0.03	0.04	0.03	0.22
Thauera mechernichensis / humireducens (100 %)	0.01	0.00	0.00	0.22
Dialister propionicifaciens / Dialister succinatiphilus YIT 11850 (98.41 %)	0.00	0.00	0.00	0.22
Nitratiruptor tergarcus DSM 16512 (85.10 %)	0.00	0.00	0.00	0.21
Pelistega suis (98.42 %)	0.00	0.01	0.00	0.20

5.5. Antibiotic Resistance Genes Profiles in the AnMBR Samples

ARG concentrations were determined by qPCR on extracted DNA from the effluents and membranes samples during phase II of the experiment for both LPD and HPD membranes at day 50 and were done in triplicates. Results showed that all HPD membrane effluents ARG concentrations were higher than that of the LPD membrane effluents, except for *tetC* (Figure 18). *intI1*, *sul1*, and *sul2* showed the highest concentrations at 4.5 $x10^{10}$copies/100 mL, 3.1 $x10^{10}$ copies/100 mL, and 8.4 $x10^{08}$ copies / 100 mL, respectively. *ampC, blaTEM, tetQ, and tetC,* had average ARGs concentrations of 6.5 $x10^{07}$ copies/ 100 mL, 2.6 $x10^{05}$ copies/100 mL, 5.3 $x10^{04}$ copies/100 mL and 2.0 $x10^{05}$ copies/100 mL, respectively. Effluent concentrations of *sul1*, *intI1*, and *sul2* seem to be unaffected by the operating conditions subjected to the reactor since no major changes were observed between the HPD and LPD membranes effluents. Instead, the effluents gene copy numbers were in parallel and in similar order of magnitude. In fact, previous studies reported a correlation between *intlI* abundance with *sul1* and *sul2* because plasmids containing such genes are conjugative in nature, enabling horizontal gene transfer. It was previously reported that genes conferring resistance to sulfonamides were present on *intl1* containing plasmids (Frank et al., 2007; Wu et al., 2010). Previous studies detected target ARGs copies similar to the ones studied in this work, to be in the ranges of 10^{04}-10^{08} copies / 100 mL (Zarei-Baygi et al. 2019; Zarei-Baygi et al. 2020b; Lou et al. 2020). Moreover, results showed that ARGs behaviors and dynamics may be different based on their nature. For example, tetracycline related resistance genes, namely *tetQ* and *tetC,* seemed to follow a similar trend considering the concentration ranges observed, whereas *intI1* and *sul1* concentrations are closer to each other than other target

ARGs, regardless of the sample. Studies that tackle ARGs proliferation are still in their early phases, yet these observations showed that the dynamics of ARGs activities is complex and not necessarily related to the operating conditions of the AnMBR.

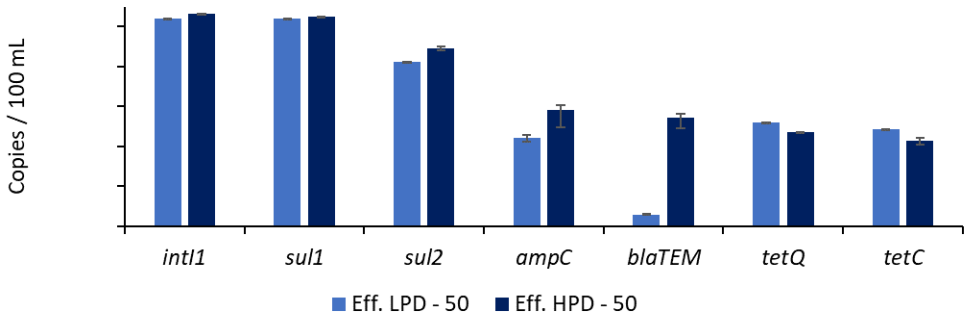

Figure 18 Antibiotic resistance gene (ARG) and intI1 gene copy abundances detected in the effluents at the end of the experiment. LPD and HPD represent the low and high pre-development membrane biofilm, respectively.

As for the membranes, a comparison between the tight and loose layers of the LPD and HPD membranes revealed different abundances in ARGs. Concentrations of *intI1*, *sul1*, *sul2*, *tetQ*, and *tetC* were the highest on the tight layer of the HPD membrane, with values of 1.08 $x10^{07}$ copies /cm^2, 4.65 $x10^{08}$ copies/ cm^2, 1.68 $x10^{07}$ copies/ cm^2, 9.89 $x10^{04}$ copies/ cm^2, and 1.17 $x10^{05}$ copies / cm^2, respectively. However, the tight layer of the LPD membrane had higher ARGs concentrations than the loose layer of the LPD membrane for *sul1*, *sul2*, *tetQ*, *blaTEM*, *tetC*, and *ampC*, with concentrations: 2.96 x 10^{08} copies / cm^2, 1.70 x 10^{06} copies / cm^2, 8.01 x 10^{04} copies / cm^2, 1.98 x 10^{04} copies / cm^2, 1.49 x 10^{06} copies / cm^2, respectively (Figure 19). A possible explanation for the higher abundance of these ARGs on the tight layers is their partial retention by the membrane. Furthermore, the development conditions of HPD membrane, i.e. high pressure, could have exercised a selective

pressure on the target ARGs (except for *ampC*) which lead to their higher retention on the HPD membrane. It is noteworthy to consider potential pathogenic groups that were reported, and some groups found highest on the tight layer of the HPD membrane. In their study, Zarei-Baygi et al. observed strong correlations between microbial community structure and ARGs concentrations. In fact, they identified that groups related to *Firmicutes, Anaerolineaceae, Clostridiales*, and *Verrucomicrobia* as potential multi-resistant host bacteria. More specifically, genera related to *Comamonas, Sulfuricurvum,* and *Flavobacterium,* which were observed in highest abundane on the tight layer of the HPD membrane, were found to strongly correlate with *sul1, sul2,* and *intl1*. Thus, known as potential hosts, it is likely that these groups were responsible for the highest gene copies number observed on that membrane. It is also possible that their higher abundance on the tight layer along with the presence of the microbial groups observed resulted in increased release of certain genes to the effluent.

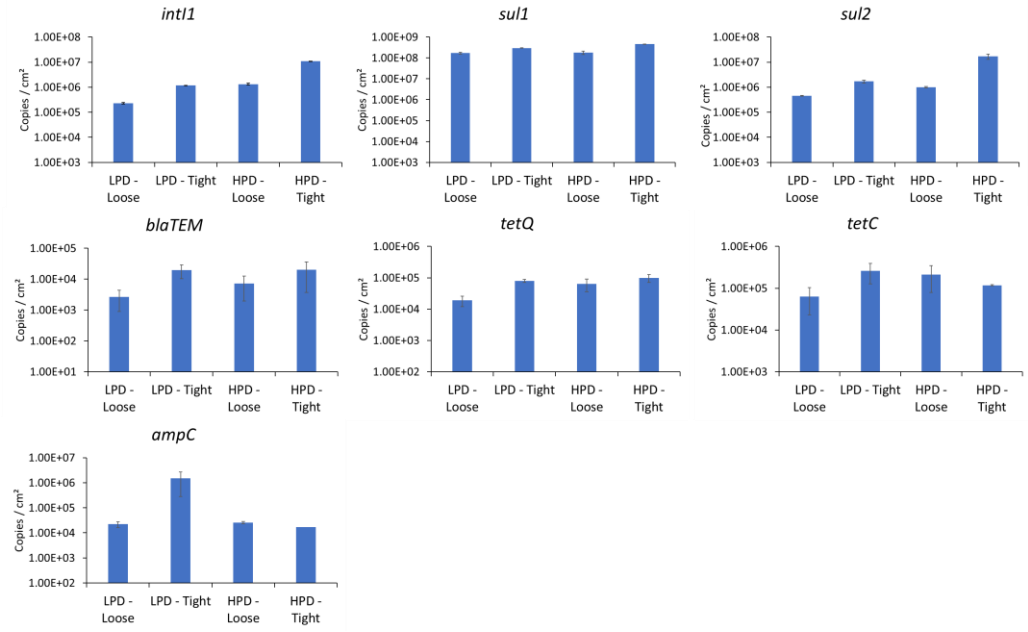

Figure 19 Antibiotic resistance gene (ARG) and *intl1* gene copy abundances detected in the AnMBR biofilm samples. LPD and HPD represent the Low and high pre-development membrane biofilm, respectively.

Chapter Six

Discussion

The main objective of this study was to devise a strategy to develop, retain, and test a membrane biofilm and determine its effect on the performance in the AnMBR. Flux variation was the parameter adopted for biofilm formation and flux rates were chosen as representative of low, medium, and high rates. Among the strategies that were tested, the membrane biofilm developed initially at the highest flux rate, resulting in the highest TMP, confirmed that there are instances where a biofilm layer could be formed and maintained on the membrane without TMP increase upon reduced operating flux. For that matter, the high TMP applied resulted in enhanced adhesion on the membrane surface, favoring EPS accumulation, namely proteins content, which were the major constituents of the biofilm. However, the threshold at which the TMP could be considered effective remains unknown and further studies are needed to test the minimum TMP required for the biofilm development and retention. In addition, it was observed that the layer was a result of a bio-cake formed since permeability and TMP were recovered when the flux was reduced on the same membrane. Furthermore, unique OTUs, among which key anaerobic fermenters, syntrophs, exoelectrogens, and methanogens, were perceived in higher abundances on the membrane. These groups were specifically linked to enhanced effluent quality. Thus, a biofilm matrix with favorable characteristics was successfully devised. It was comprised of a biocake layer, with higher concentrations of proteins, retained on the membrane, on which selected microbial groups were able to attach. The effect of transmembrane pressure on the formation and aggregation to the membrane was

found further to play a role in the stabilization of microorganisms. The active biofilm matrix formed could overall facilitate substrate utilization and eventually biodegradation of OMPs.

Recent developments in the dynamics that govern biofilm formation in the AnMBR help overcoming challenges that prevent its application to full-scale. Indeed, the role of AnMBR as an emerging technology for wastewater treatment is found to include additional advantages to its already known benefits in terms higher effluent quality recovered. This advantage lies in the possibility of removing recalcitrant OMPs for a safer reuse of the effluent. Furthermore, the new approach to anaerobic membrane biofilms formation established in this work contributes greatly to the sustainability of the technology.

Regarding sustainability aspects, AnMBRs should be both process and effluent efficient to support advancing the technology. The treatment process should be less energy intensive, and the effluent recovered should be more regulated in terms of pathogens and chemical contaminants presence. For that matter, the ability to recover and maintain TMP has always been an issue (as it was discussed in the previous sections), specially that it was previously perceived that the formation of a dense membrane biofilm causes increases in TMP. The controlled strategy for biofilm development presented in this work offered the possibility of reducing further the operating costs regarding AnMBRs. An initial high TMP would be required to form the biofilm layer and ensure its stability, after which TMP could be reduced during the operation, requiring less energy. In addition, the dissociation between TMP and biofilm formation paves the way for more research to focus on understanding the effect of operation conditions of the AnMBR in general. As for the effluent, the controlled biofilm matrix promoted OMPs removal through the enhancement of a

selective consortia capable to be maintained under varying operating conditions on the membrane.

It is clear that devising a strategy for membrane biofilm was feasible and the benefits were highlighted in the study. However, less advantageous outcomes should not be overlooked. It is noteworthy that higher dissolved methane contents were observed on the membrane developed at high pressure initially. This was a result of higher COD removal attributed to specific microbial groups found at higher abundances on that membrane. Moreover, higher ARG concentrations were found in the effluent of the HPD membrane. The high pressure could have aided certain ARGs to pass through the membrane and couldn't be retained.

The present work aimed at devising and testing a strategy for anaerobic membrane biofilm development. However, one of the limitations of the study is the treatment of synthetic wastewater, which is not representative of real-world application if AnMBR is to be considered for full-scale application. Moreover, only one membrane type was used, on which the biofilm was allowed to develop. Other types of membranes, such as ultrafiltration with different pore sizes, could present different biofilm development dynamics. The development of the membrane biofilm in this study was only tested on a AnMBR-CSTR, and replication on other types of filtration media was not envisaged.

Chapter Seven

Conclusions

AnMBRs have been identified as an emerging technology for the treatment of wastewater based on energy recovery, reusable permeate, and removal of emerging contaminants. Moreover, membrane biofilm has been recently shown to possess advantages that add to the existing benefits of AnMBRs. The experiment focused on testing different membrane biofilms developed under various conditions, in phases I and II, respectively. The present work suggested that controlled membrane biofilm development at transmembrane pressures near critical flux can be subsequently operable at lower flux rates without significant re-emergence of TMP build-up. In addition, a positive relation between high pressure conditions and the growth of unique microbial communities was identified. Methanogens and syntrophic microbial groups interaction improved effluent quality without deteriorating the performance of the AnMBR, while enhancing micropollutants removal. Thus, targeted biofilm development has notable implications for reducing the threat of emerging contaminants from wastewater discharges. The study is the first (to the authors' knowledge) to delineate membrane biofilm development conditions that can potentially be sustainable for operation while also promoting better effluent quality. The work also contributes to understanding the interactions of key anaerobic microbial groups with the fate of emerging contaminants in AnMBR systems, which ultimately decrease challenges that hinder the adoption of the AnMBR for full-scale wastewater treatment.

7.1. Future Work

Targeted research for advancing the role of membrane biofilms in providing increased organic matter and OMPs removal is still in its early stages. As the advantages of a membrane biofilm have only been recently acknowledged, further research should focus on devising strategies that promote the development of the membrane biofilm over extended durations for the sustainability of the process. Since higher dissolved methane concentrations were observed on the membrane developed at the highest pressure, effluent methane recovery techniques are to be considered as part of future work. In order to elucidate real conditions, membrane biofilm development strategies should include real wastewater treatment as they are more complex.

References

.

Amin, F. R., Khalid, H., El-Mashad, H. M., Chen, C., Liu, G., & Zhang, R. (2021). Functions of bacteria and archaea participating in the bioconversion of organic waste for methane production. *Science of The Total Environment*, *763*, 143007.

Altschul S. F., Gish W., Miller W., Myers E. W. and Lipman D. J. (1990). Basic local alignment search tool. *Journal of molecular biology* **215**(3), 403-10.

Alvarino, T., Suarez, S., Lema, J. M., & Omil, F. (2014). Understanding the removal mechanisms of PPCPs and the influence of main technological parameters in anaerobic UASB and aerobic CAS reactors. Journal of hazardous materials, 278, 506-513.

Aziz, A., Sengar, A., Basheer, F., Farooqi, I. H., & Isa, M. H. (2022). Anaerobic digestion in the elimination of antibiotics and antibiotic-resistant genes from the environment–A comprehensive review. *Journal of Environmental Chemical Engineering*, *10*(1), 106423.

Baek, S. H., & Pagilla, K. R. (2006). Aerobic and anaerobic membrane bioreactors for municipal wastewater treatment. Water environment research, 78(2), 133-140.

Baird R., Eaton A. and Rice E. (2005). 2540 SOLIDS. In: *Standard methods for the examination of water and wastewater*, American Public Health Association.

Baquero, F., Martínez, J. L., & Cantón, R. (2008). Antibiotics and antibiotic resistance in water environments. Current opinion in biotechnology, 19(3), 260-265.

Barlow, R.S., Pemberton, J.M., Desmarchelier, P.M., Gobius, K.S., 2004. Isolation and characterization of integron-containing bacteria without antibiotic selection. Antimicrobial agents and chemotherapy 48, 838-842.

Belfort, G., Davis, R. H., & Zydney, A. L. (1994). The behavior of suspensions and macromolecular solutions in crossflow microfiltration. Journal of membrane science, 96(1-2), 1-58. Applied and Environmental Microbiology 73, 4785-4790.

Bibbal, D., Dupouy, V., Ferré, J.-P., Toutain, P.-L., Fayet, O., Prère, M.-F., Bousquet-Mélou, A., 2007. Impact of three ampicillin dosage regimens on selection of ampicillin resistance in Enterobacteriaceae and excretion of blaTEM genes in swine feces.

Charfi, A., Amar, N. B., & Harmand, J. (2012). Analysis of fouling mechanisms in anaerobic membrane bioreactors. Water research, 46(8), 2637-2650.

Chen H. and Zhang M. (2013). Occurrence and removal of antibiotic resistance genes in municipal wastewater and rural domestic sewage treatment systems in eastern China. *Environment international* **55**, 9-14.

Chen, J., Tong, T., Jiang, X., & Xie, S. (2020). Biodegradation of sulfonamides in both oxic and anoxic zones of vertical flow constructed wetland and the potential degraders. Environmental Pollution, 265, 115040.

Chen, Q., Wu, W., Qi, D., Ding, Y., & Zhao, Z. (2020). Review on microaeration-based anaerobic digestion: state of the art, challenges, and prospectives. Science of the Total Environment, 710, 136388.

Cheng, H., Cheng, D., Mao, J., Lu, T., & Hong, P. Y. (2019). Identification and characterization of core sludge and biofilm microbiota in anaerobic membrane bioreactors. Environment international, 133, 105165.

Cheng, H., & Hong, P. Y. (2017). Removal of antibiotic-resistant bacteria and antibiotic resistance genes affected by varying degrees of fouling on anaerobic microfiltration membranes. Environmental science & technology, 51(21), 12200-12209.

Chopra I. and Roberts M. (2001). Tetracycline antibiotics: mode of action, applications, molecular biology, and epidemiology of bacterial resistance. *Microbiology and molecular biology reviews* **65**(2), 232-60.

Dahllöf, I., Baillie, H., Kjelleberg, S., 2000. rpoB-based microbial community analysis avoids limitations inherent in 16S rRNA gene intraspecies heterogeneity. Applied and environmental microbiology 66, 3376-3380.

Dagnew, M., & Parker, W. (2021). Impact of AnMBR operating conditions on anaerobic digestion of waste activated sludge. Water Environment Research, 93(5), 703-713.

Dong, D., Choi, O. K., & Lee, J. W. (2022). Influence of the continuous addition of zero valent iron (ZVI) and nano-scaled zero valent iron (nZVI) on the anaerobic biomethanation of carbon dioxide. *Chemical Engineering Journal*, *430*, 132233.

Du, J., Geng, J., Ren, H., Ding, L., Xu, K., & Zhang, Y. (2015). Variation of antibiotic resistance genes in municipal wastewater treatment plant with

A2O-MBR system. Environmental Science and Pollution Research, 22(5), 3715-3726.

Dubois, M., Gilles, K. A., Hamilton, J. K., Rebers, P. T., & Smith, F. (1956). Colorimetric method for determination of sugars and related substances. *Analytical chemistry*, *28*(3), 350-356.

Schwarzenbach, R. P., Escher, B. I., Fenner, K., Hofstetter, T. B., Johnson, C. A., Von Gunten, U., & Wehrli, B. (2006). The challenge of micropollutants in aquatic systems. *Science*, *313*(5790), 1072-1077.

Ding, Y., Tian, Y., Li, Z., Zuo, W., & Zhang, J. (2015). A comprehensive study into fouling properties of extracellular polymeric substance (EPS) extracted from bulk sludge and cake sludge in a mesophilic anaerobic membrane bioreactor. Bioresource technology, 192, 105-114.

Frank, T., Gautier, V., Talarmin, A., Bercion, R., & Arlet, G. (2007). Characterization of sulphonamide resistance genes and class 1 integron gene cassettes in Enterobacteriaceae, Central African Republic (CAR). Journal of Antimicrobial Chemotherapy, 59(4), 742-745.

Fujimoto, M., Carey, D. E., Zitomer, D. H., & McNamara, P. J. (2019). Syntroph diversity and abundance in anaerobic digestion revealed through a comparative core microbiome approach. *Applied microbiology and biotechnology*, *103*(15), 6353-6367.

Gonzalez-Gil, L., Carballa, M., & Lema, J. M. (2017). Cometabolic enzymatic transformation of organic micropollutants under methanogenic conditions. Environmental science & technology, 51(5), 2963-2971.

Gonzalez-Gil, L., Mauricio-Iglesias, M., Serrano, D., Lema, J. M., & Carballa, M. (2018). Role of methanogenesis on the biotransformation of organic micropollutants during anaerobic digestion. *Science of the Total Environment*, *622*, 459-466.

Gouveia, J., Plaza, F., Garralon, G., Fdz-Polanco, F., & Peña, M. (2015). Long-term operation of a pilot scale anaerobic membrane bioreactor (AnMBR) for the treatment of municipal wastewater under psychrophilic conditions. Bioresource Technology, 185, 225-233.

Hai, F. I., Yamamoto, K., & Lee, C. H. (Eds.). (2018). Membrane biological reactors: theory, modeling, design, management and applications to wastewater reuse. Iwa Publishing.

Harb, M., Xiong, Y., Guest, J., Amy, G., & Hong, P. Y. (2015a). Differences in microbial communities and performance between suspended and attached growth anaerobic membrane bioreactors treating synthetic municipal wastewater. *Environmental Science: Water Research & Technology*, *1*(6), 800-813.

Harb, M., Xiong, Y., Guest, J., Amy, G., & Hong, P. Y. (2015b). Differences in microbial communities and performance between suspended and attached growth anaerobic membrane bioreactors treating synthetic municipal wastewater. *Environmental Science: Water Research & Technology*, *1*(6), 800-813.

Harb, M., & Hong, P. Y. (2017). Anaerobic membrane bioreactor effluent reuse: A review of microbial safety concerns. Fermentation, 3(3), 39.

Harb, M., Lou, E., Smith, A. L., & Stadler, L. B. (2019). Perspectives on the fate of micropollutants in mainstream anaerobic wastewater treatment. *Current opinion in biotechnology*, *57*, 94-100.

Harb, M., Zarei-Baygi, A., Wang, P., Sawaya, C. B., McCurry, D. L., Stadler, L. B., & Smith, A. L. (2021). Antibiotic transformation in an anaerobic membrane bioreactor linked to membrane biofilm microbial activity. *Environmental Research*, *200*, 111456.

Hwang, B. K., Lee, W. N., Yeon, K. M., Park, P. K., Lee, C. H., Chang, I. S., ... & Kraume, M. (2008). Correlating TMP increases with microbial characteristics in the bio-cake on the membrane surface in a membrane bioreactor. Environmental science & technology, 42(11), 3963-3968.

Ileleji, K. E., Martin, C., & Jones, D. (2015, January). Basics of energy production through anaerobic digestion of livestock manure. In Bioenergy (pp. 287-295). Academic Press.

Jain, S., Jain, S., Wolf, I. T., Lee, J., & Tong, Y. W. (2015). A comprehensive review on operating parameters and different pretreatment methodologies for anaerobic digestion of municipal solid waste. Renewable and Sustainable Energy Reviews, 52, 142-154.

Jefferson, B., Laine, A. L., Judd, S. J., & Stephenson, T. (2000). Membrane bioreactors and their role in wastewater reuse. Water Science and Technology, 41(1), 197-204.

Jeswani, H. K., & Azapagic, A. (2011). Water footprint: methodologies and a case study for assessing the impacts of water use. Journal of cleaner production, 19(12), 1288-1299.

Jia, Y., Zhang, H., Khanal, S. K., Yin, L., & Lu, H. (2019). Insights into pharmaceuticals removal in an anaerobic sulfate-reducing bacteria sludge system. Water research, 161, 191-201.

Judd, S. J. (2016). The status of industrial and municipal effluent treatment with membrane bioreactor technology. Chemical Engineering Journal, 305, 37-45.

Kabaivanova, L., Hubenov, V., Dimitrova, L., Simeonov, I., Wang, H., & Petrova, P. (2022). Archaeal and Bacterial Content in a Two-Stage Anaerobic System for Efficient Energy Production from Agricultural Wastes. *Molecules*, *27*(5), 1512.

Kappell, A. D., Kimbell, L. K., Seib, M. D., Carey, D. E., Choi, M. J., Kalayil, T., ... & McNamara, P. J. (2018). Removal of antibiotic resistance genes in an anaerobic membrane bioreactor treating primary clarifier effluent at 20 C. Environmental Science: Water Research & Technology, 4(11), 1783-1793.

Kim, M., Ahn, Y. H., & Speece, R. E. (2002). Comparative process stability and efficiency of anaerobic digestion; mesophilic vs. thermophilic. Water research, 36(17), 4369-4385.

Kiran, E. U., Stamatelatou, K., Antonopoulou, G., & Lyberatos, G. (2016). Production of biogas via anaerobic digestion. In *Handbook of Biofuels Production* (pp. 259-301). Woodhead Publishing.

Kong, Q., He, X., Ma, S. S., Feng, Y., Miao, M. S., Xu, F., & Wang, Q. (2017). The performance and evolution of bacterial community of activated sludge exposed to trimethoprim in a sequencing batch reactor. *Bioresource technology*, *244*, 872-879.

Kozich J. J., Westcott S. L., Baxter N. T., Highlander S. K. and Schloss P. D. (2013). Development of a dual-index sequencing strategy and curation pipeline for analyzing amplicon sequence data on the MiSeq Illumina sequencing platform. *Applied and environmental microbiology* **79**(17), 5112-20.

Le, T. H., Ng, C., Tran, N. H., Chen, H., & Gin, K. Y. H. (2018). Removal of antibiotic residues, antibiotic resistant bacteria and antibiotic resistance genes in municipal wastewater by membrane bioreactor systems. Water research, 145, 498-508.

Liang, B., Kong, D., Qi, M., Yun, H., Li, Z., Shi, K., ... & Wang, A. (2019). Anaerobic biodegradation of trimethoprim with sulfate as an electron acceptor. *Frontiers of Environmental Science & Engineering*, *13*(6), 1-10.

Liao, B. Q., Kraemer, J. T., & Bagley, D. M. (2006). Anaerobic membrane bioreactors: applications and research directions. Critical Reviews in Environmental Science and Technology, 36(6), 489-530.

Lin, H. J., Xie, K., Mahendran, B., Bagley, D. M., Leung, K. T., Liss, S. N., & Liao, B. Q. (2009). Sludge properties and their effects on membrane fouling in submerged anaerobic membrane bioreactors (SAnMBRs). Water Research, 43(15), 3827-3837.

Liu, Z. H., Yin, H., Dang, Z., & Liu, Y. (2014). Dissolved methane: a hurdle for anaerobic treatment of municipal wastewater.

Lou E. G., Harb M., Smith A. L. and Stadler L. B. (2020). Livestock manure improved antibiotic resistance gene removal during co-treatment of domestic wastewater in an anaerobic membrane bioreactor. Environmental Science: Water Research & Technology 6(10), 2832-42.

Luste, S., & Luostarinen, S. (2010). Anaerobic co-digestion of meat-processing by-products and sewage sludge–Effect of hygienization and organic loading rate. Bioresource Technology, 101(8), 2657-2664.

Matar, G. K., Bagchi, S., Zhang, K., Oerther, D. B., & Saikaly, P. E. (2017). Membrane biofilm communities in full-scale membrane bioreactors are not randomly assembled and consist of a core microbiome. *Water research*, *123*, 124-133.

Maaz, M., Yasin, M., Aslam, M., Kumar, G., Atabani, A. E., Idrees, M., ... & Kim, J. (2019). Anaerobic membrane bioreactors for wastewater treatment: Novel configurations, fouling control and energy considerations. Bioresource technology, 283, 358-372.

Massé, A., Spérandio, M., & Cabassud, C. (2006). Comparison of sludge characteristics and performance of a submerged membrane bioreactor and an activated sludge process at high solids retention time. *Water research*, *40*(12), 2405-2415.

Mao, C., Feng, Y., Wang, X., & Ren, G. (2015). Review on research achievements of biogas from anaerobic digestion. Renewable and sustainable energy reviews, 45, 540-555.

Miller, G. W. (2006). Integrated concepts in water reuse: managing global water needs. Desalination, 187(1-3), 65-75.

Monsalvo, V. M., McDonald, J. A., Khan, S. J., & Le-Clech, P. (2014). Removal of trace organics by anaerobic membrane bioreactors. Water Research, 49, 103-112.

Naas, T., Ergani, A., Carrër, A., Nordmann, P., 2011. Real-time PCR for detection of NDM-1 carbapenemase genes from spiked stool samples. Antimicrobial agents and chemotherapy 55, 4038-4043.

Namkung, E., & Rittmann, B. E. (1986). Soluble microbial products (SMP) formation kinetics by biofilms. Water Research, 20(6), 795-806.

Ng, H. Y., Tan, T. W., & Ong, S. L. (2006). Membrane fouling of submerged membrane bioreactors: impact of mean cell residence time and the contributing factors. Environmental science & technology, 40(8), 2706-2713.

Pei, R., Kim, S.-C., Carlson, K.H., Pruden, A., 2006. Effect of river landscape on the sediment concentrations of antibiotics and corresponding antibiotic resistance genes (ARG). Water research 40, 2427-2435.

Quast C., Pruesse E., Yilmaz P., Gerken J., Schweer T., Yarza P., Peplies J. and Glöckner F. O. (2012). The SILVA ribosomal RNA gene database project: improved data processing and web-based tools. *Nucleic acids research* **41**(D1), D590-D6.

Robles, Á., Durán, F., Giménez, J. B., Jiménez, E., Ribes, J., Serralta, J., ... & Rogalla, F. (2020). Anaerobic membrane bioreactors (AnMBR) treating urban wastewater in mild climates. Bioresource Technology, 314, 123763.

Saia, F. T., Souza, T. S., Duarte, R. T. D., Pozzi, E., Fonseca, D., & Foresti, E. (2016). Microbial community in a pilot-scale bioreactor promoting anaerobic digestion and sulfur-driven denitrification for domestic sewage treatment. Bioprocess and biosystems engineering, 39(2), 341-352.

Sanguanpak, S., Chiemchaisri, W., & Chiemchaisri, C. (2019). Membrane fouling and micro-pollutant removal of membrane bioreactor treating landfill leachate. Reviews in Environmental Science and Bio/Technology, 18(4), 715-740.

Schloss P. D., Westcott S. L., Ryabin T., Hall J. R., Hartmann M., Hollister E. B., Lesniewski R. A., Oakley B. B., Parks D. H. and Robinson C. J. (2009). Introducing mothur: open-source, platform-independent, community-

supported software for describing and comparing microbial communities. *Applied and environmental microbiology* **75**(23), 7537-41.

Schwarzenbach, R. P., Escher, B. I., Fenner, K., Hofstetter, T. B., Johnson, C. A., von Gunten, U., & Wehrli, B. (2006). The challenge of micropollutants in aquatic systems. Science, 313(5790), 1072-1077. https://doi.org/10.1126/science.1127291

Smith, A. L., Stadler, L. B., Love, N. G., Skerlos, S. J., & Raskin, L. (2012). Perspectives on anaerobic membrane bioreactor treatment of domestic wastewater: a critical review. Bioresource technology, 122, 149-159.

Sui, Q., Cao, X., Lu, S., Zhao, W., Qiu, Z., & Yu, G. (2015). Occurrence, sources and fate of pharmaceuticals and personal care products in the groundwater: a review. *Emerging Contaminants*, *1*(1), 14-24.

Szczepanowski, R., Linke, B., Krahn, I., Gartemann, K.-H., Gützkow, T., Eichler, W., Pühler, A., Schlüter, A., 2009. Detection of 140 clinically relevant antibiotic-resistance genes in the plasmid metagenome of wastewater treatment plant bacteria showing reduced susceptibility to selected antibiotics. Microbiology 155, 2306-2319.

Trzcinski, A. P., & Stuckey, D. C. (2010). Treatment of municipal solid waste leachate using a submerged anaerobic membrane bioreactor at mesophilic and psychrophilic temperatures: analysis of recalcitrants in the permeate using GC-MS. water research, 44(3), 671-680.

Van, D. P., Fujiwara, T., Tho, B. L., Toan, P. P. S., & Minh, G. H. (2020). A review of anaerobic digestion systems for biodegradable waste: Configurations, operating parameters, and current trends. *Environmental Engineering Research*, *25*(1), 1-17.

Vásquez, E., Trapote, A., & Prats, D. (2018). Elimination of pesticides with a membrane bioreactor and two different sludge retention times. Tecnología y ciencias del agua, 9(5), 198-217.

Venkataraman, A., Rosenbaum, M. A., Perkins, S. D., Werner, J. J., & Angenent, L. T. (2011). Metabolite-based mutualism between Pseudomonas aeruginosa PA14 and Enterobacter aerogenes enhances current generation in bioelectrochemical systems. Energy & Environmental Science, 4(11), 4550-4559.

Ventola, C. L. (2015). The antibiotic resistance crisis: part 1: causes and threats. Pharmacy and therapeutics, 40(4), 277.

Verbeeck, K., Buelens, L. C., Galvita, V. V., Marin, G. B., Van Geem, K. M., & Rabaey, K. (2018). Upgrading the value of anaerobic digestion via chemical production from grid injected biomethane. Energy & Environmental Science, 11(7), 1788-1802.

Viswanathan, V. K. (2014). Off-label abuse of antibiotics by bacteria. Gut Microbes, 5(1), 3-4.

Vrouwenvelder, J. S., Kruithof, J. C., & Van Loosdrecht, M. C. M. (2010). Integrated approach for biofouling control. Water science and technology, 62(11), 2477-2490.

Wang Q., Garrity G. M., Tiedje J. M. and Cole J. R. (2007). Naive Bayesian classifier for rapid assignment of rRNA sequences into the new bacterial taxonomy. *Applied and environmental microbiology* **73**(16), 5261-7.

Wang, S., Ma, F., Ma, W., Wang, P., Zhao, G., & Lu, X. (2019). Influence of temperature on biogas production efficiency and microbial community in a two-phase anaerobic digestion system. *Water*, *11*(1), 133.

Weiß, S., Lebuhn, M., Andrade, D., Zankel, A., Cardinale, M., Birner-Grünberger, R., ... & Guebitz, G. M. (2013). Activated zeolite—suitable carriers for microorganisms in anaerobic digestion processes?. *Applied microbiology and biotechnology*, *97*(7), 3225-3238.

Wijekoon, K. C., McDonald, J. A., Khan, S. J., Hai, F. I., Price, W. E., & Nghiem, L. D. (2015). Development of a predictive framework to assess the removal of trace organic chemicals by anaerobic membrane bioreactor. *Bioresource technology*, *189*, 391-398.

Wu, S., Dalsgaard, A., Hammerum, A. M., Porsbo, L. J., & Jensen, L. B. (2010). Prevalence and characterization of plasmids carrying sulfonamide resistance genes among Escherichia coli from pigs, pig carcasses and human. Acta Veterinaria Scandinavica, 52(1), 1-7.

Wu, L., Yang, Y., Chen, S. I., Zhao, M., Zhu, Z., Yang, S., ... & He, Q. (2016). Long-term successional dynamics of microbial association networks in anaerobic digestion processes. *Water research*, *104*, 1-10.

Xiong, Y., Harb, M., & Hong, P. Y. (2016). Characterization of biofoulants illustrates different membrane fouling mechanisms for aerobic and anaerobic membrane bioreactors. Separation and Purification Technology, 157, 192-202.

Yao, Y., Zhou, Z., Stuckey, D. C., & Meng, F. (2020). Micro-particles—a neglected but critical cause of different membrane fouling between aerobic and anaerobic membrane bioreactors. ACS Sustainable Chemistry & Engineering, 8(44), 16680-16690.

Yao, Y., Xu, R., Zhou, Z., & Meng, F. (2021). Linking dynamics in morphology, components, and microbial communities of biocakes to fouling evolution: a comparative study of anaerobic and aerobic membrane bioreactors. Chemical Engineering Journal, 413, 127483.

Zamorano-López, N., Borrás, L., Giménez, J. B., Seco, A., & Aguado, D. (2019). Acclimatised rumen culture for raw microalgae conversion into biogas: Linking microbial community structure and operational parameters in anaerobic membrane bioreactors (AnMBR). *Bioresource Technology*, *290*, 121787.

Zarei-Baygi, A., Harb, M., Wang, P., Stadler, L. B., & Smith, A. L. (2020). Microbial community and antibiotic resistance profiles of biomass and effluent are distinctly affected by antibiotic addition to an anaerobic membrane bioreactor. *Environmental Science: Water Research & Technology*, *6*(3), 724-736.

Zarei-Baygi, A., Wang, P., Harb, M., Stadler, L. B., & Smith, A. L. (2020). Membrane fouling inversely impacts intracellular and extracellular antibiotic resistance gene abundances in the effluent of an anaerobic membrane bioreactor. Environmental Science & Technology, 54(19), 12742-12751.

Zhang, S., Zhou, Z., Li, Y., & Meng, F. (2018). Deciphering the core fouling-causing microbiota in a membrane bioreactor: low abundance but important roles. Chemosphere, 195, 108-118.

Zhou Z.-C., Feng W.-Q., Han Y., Zheng J., Chen T., Wei Y.-Y., Gillings M., Zhu Y.-G. and Chen H. (2018). Prevalence and transmission of antibiotic resistance and microbiota between humans and water environments. *Environment international* **121**, 1155-61.

.

Appendix A

Synthetic wastewater composition

Table 1 Synthetic wastewater composition used during the experiment (1500 mg. COD/L)

Concentrate solution		Dilution water	
Reagent	Conc. (mg/L)	Reagent	Conc. (mg/L)
Ammonium Chloride	17.5	Sodium Bicarbonate	420
Calcium Chloride	18.1	Sodium Carbonate	420
Iron Sulfate	9.1	Potassium Phosphate	36.1
Sodium Sulfate	18.1		
Sodium Acetate	481.8		
Peptone	63.8		
Yeast	191.1		
Milk Powder	283.4		
Starch	446.5		
Copper Chloride	6.25		
Manganese Sulfate	1.3		
Lead Chloride	5		

Theoretical COD Calculation

The COD contribution of the synthetic wastewater mentioned is calculated as follow:

1. The COD contribution of the constituents was calculated based on stoichiometric equation assuming total conversion of O_2:

Starch:

$$C_{6H_{10}O_5} + 6O_2 \rightarrow 6CO_2 + 5H_2O$$

$$\left(162\frac{g}{mol}\right) + \left(192\frac{g}{mol}\right) \rightarrow \left(44\frac{g}{mol}\right) + \left(18\frac{g}{mol}\right)$$

1.185 g. COD per g. starch

Carbohydrates:

$$CH_2O + O_2 \rightarrow CO_2 + H_2O$$

$$\left(30\frac{g}{mol}\right) + \left(32\frac{g}{mol}\right) \rightarrow \left(44\frac{g}{mol}\right) + \left(18\frac{g}{mol}\right)$$

1.067 g. of COD per g. of carbohydrates

Lipids:

$$C_{16}H_{32}O_2 + 23O_2 \rightarrow 16CO_2 + 16H_2O$$

$\left(256\frac{g}{mol}\right) + \left(736\frac{g}{mol}\right) \rightarrow \left(44\frac{g}{mol}\right) + (18\frac{g}{mol})$

2.875 g of COD per gram of lipid

Proteins:

$C_{16}H_{24}O_5N_4 + O_2 \rightarrow 16CO_2 + 12H_2O$

1.50 g. of COD per gram of protein was assumed

Sodium acetate:

$2CH_3COONa + 4O_2 \rightarrow Na_2CO_3 + 3CO_2 + 3H_2O$

$\left(164\frac{g}{mol}\right) + \left(123\frac{g}{mol}\right) \rightarrow \left(106\frac{g}{mol}\right) + \left(44\frac{g}{mol}\right) + (18\frac{g}{mol})$

Knowing that 1 g. of CH_3COONa contains 0.72 g. of CH_3COO^-,

1.85g. of COD per gram of CH_3COO^-

2. The COD contribution of each constituent was calculated based on the mass added to the synthetic feed prepared:

The milk powder constitution: 26.96% Proteins, 43.5 % Carbohydrates, 29.06% lipids.

Table 2 COD contribution of each carbon source constituent

Constituent	Mass added (mg)	Mass COD calculated (mg)
Starch	446.5	83
Milk (Proteins)	283.4	115
Milk (carbohydrates)	283.4	132
Milk (lipids)	283.4	237
Peptone (proteins)	63.8	96
Yeast (proteins)	191.1	287
Sodium acetate	481.8	523

Theoretical Biogas Production

The following stoichiometric equation was used for the maximum theoretical methane production:

$CH_4 + 2O_2 \rightarrow CO_2 + 2H_2O$

$\left(16\frac{g}{mol}\right) + \left(64\frac{g}{mol}\right) \rightarrow \left(44\frac{g}{mol}\right) + \left(36\frac{g}{mol}\right)$

Thus, 0.25 g. CH_4 for each gram COD consumed.

Total COD Mass Balance

$$COD_{influent} = COD_{effluent} + COD_{biomass} + COD_{methane}$$

- $COD_{influent} = 1.5\ g.\frac{COD}{L} \times 2.2\frac{L_{Influent}}{day} = 3.3\ g.COD/day$
- $COD_{effluent} = 21\ \frac{mg.COD}{L} \times 2.1\ L_{Effluent}/day$= 44.1 mg. COD/day
- $COD_{biomass}$:
  Growth of VSS = 1.35 g / L over 7 days; COD conversion to biomass = 1.42 g. COD / g. VSS (Rittman and McCarty, 2012); reactor level = 3L.
  Biomass growth $=\frac{1.35\ g.\frac{VSS}{L} \times 3L}{7\ days} = 0.58\ \frac{g.VSS}{day}$

- $COD_{biomass} = 0.58\ \frac{g.VSS}{day} \times 1.42\ \frac{g.COD}{g.VSS} = 0.82\ g.\frac{COD}{day}$

$$COD_{methane}(measured) = \frac{0.93\ \frac{L\ CH_4}{day}}{0.382\ \frac{L\ CH_4}{g.COD\ removed}} = 2.4\ \frac{g.CODremoved}{day}$$

Effluent methane contribution:

$$Effluent\ methane\ (measured) = 15.5\frac{mL}{Leff} \times 2.06\frac{L_{out}}{day} = 31.93\ mL_{CH_4}/day$$

$$COD_{effluent\ methane}(measured) = \frac{31.93\ \frac{mL_{CH_4}}{day}}{382\ \frac{mL\ CH_4}{g.COD\ removed}} = 0.08\ \frac{g.COD\ removed}{day}$$

Trimethoprim Characteristics

The characteristics of trimethoprim were retrieved from chemspider as follow:

Chemical Formula: $C_{14}H_{18}N_4O_3$

Molecular Weight: 290.318 g/mol

K_{OW}: 0.91

Retention time: 5.05 min

Monoisotopic mass (m/z): 290.14

Appendix B

COD Effluent concentrations Results

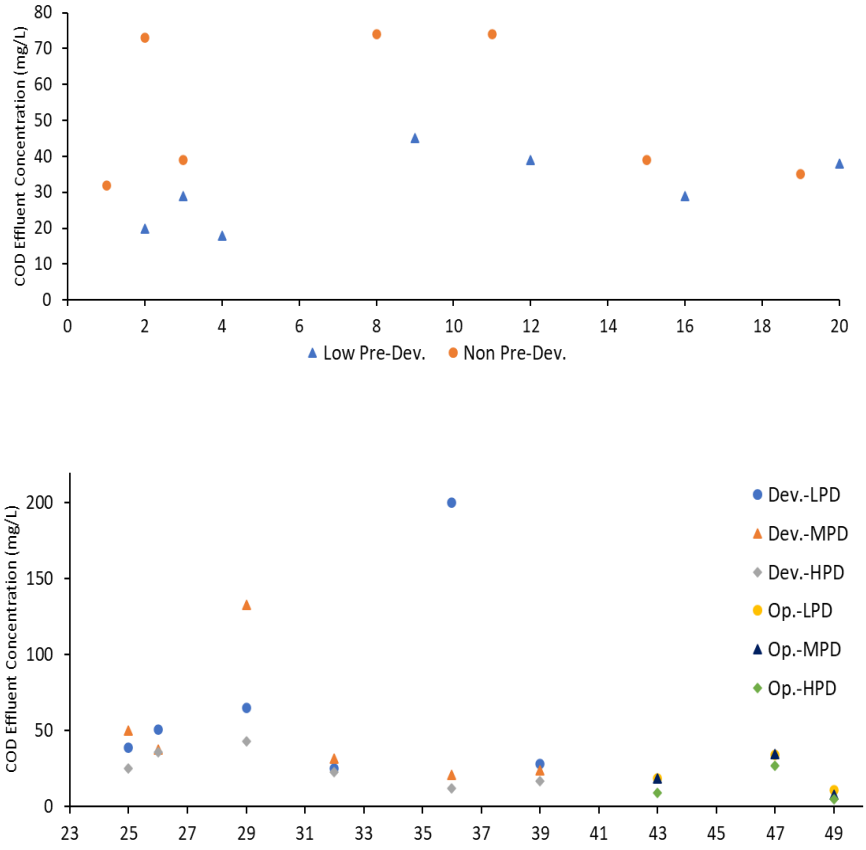

Figure 20 AnMBR effluent COD values during phase I (A) and phase II (B). Low Pre-Dev represents the membrane biofilm developed at low flux while non Pre-Dev. was operated for comparison. Dev. And Op. represent the development and operation stages of the membrane biofilms. LPD represents Low pre-developed, MPD medium pre-developed, and HPD high pre-developed.

Effluent Dissolved Methane Results

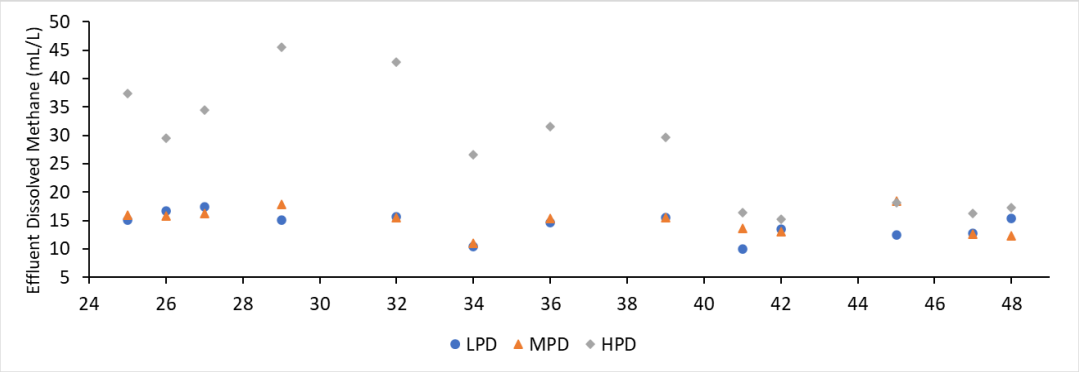

Figure 21 AnMBR effluent dissolved methane concentrations of each AnMBR membrane operated during phase II. LPD represents low pre-development. MPD represents mid pre-development. HPD represents high pre-developed